

# Some relations between Lagrangian models and synthetic random velocity fields

Piero Olla and Paolo Paradisi

ISAC-CNR, Sezione di Lecce

Str. Prov. Lecce-Monteroni Km 1.2 I-73100 Lecce, Italy

## Abstract

We propose an alternative interpretation of Markovian transport models based on the well-mixedness condition, in terms of the properties of a random velocity field with second order structure functions scaling linearly in the space time increments. This interpretation allows direct association of the drift and noise terms entering the model, with the geometry of the turbulent fluctuations. In particular, the well known non-uniqueness problem in the well-mixedness approach is solved in terms of the antisymmetric part of the velocity correlations; its relation with the presence of non-zero mean helicity and other geometrical properties of the flow is elucidated. The well-mixedness condition appears to be a special case of the relation between conditional velocity increments of the random field and the one-point Eulerian velocity distribution, allowing generalization of the approach to the transport of non-tracer quantities. Application to solid particle transport leads to a model satisfying, in the homogeneous isotropic turbulence case, all the conditions on the behaviour of the correlation times for the fluid velocity sampled by the particles. In particular, correlation times in the gravity and in the inertia dominated case, respectively, longer and shorter than in the passive tracer case; in the gravity dominated case, correlation times longer for velocity components along gravity, than for the perpendicular ones. The model has been used, in a turbulent channel flow, to isolate the effect of near-wall intermittency and anisotropic coherent structures, on the particle deposition and accumulation rates.

# I. Introduction

In Lagrangian models, the concentration of a quantity transported by a turbulent field is reconstructed from the trajectories of the individual particles advected by the flow [1, 2, 3, 4]. Since each trajectory is associated with an independent realization of the turbulent flow, what is obtained is actually the mean concentration profile, given a certain distribution of sinks and sources for the transported quantity.

One keeps into account the fact that the turbulent length and time scales are non-zero, by assuming that the particle velocity obeys a Langevin equation; this results in the system of equations, in terms of the particle Lagrangian velocity  $\mathbf{v}$  and coordinate  $\mathbf{x}$ :

$$\begin{cases} d\mathbf{x} = \mathbf{v}dt \\ d\mathbf{v} = \mathbf{a}(\mathbf{v}, \mathbf{x}, t)dt + d\mathbf{w} \\ \langle dw^i dw^j \rangle = \mathcal{B}^{ij}(\mathbf{v}, \mathbf{x}, t)dt \end{cases} \quad (1)$$

A strong physical motivation for a Lagrangian model in the form of Eqn. (1) is the linear scaling of the Lagrangian velocity structure functions for inertial range time separations [5]. In the case of passive tracers, we have

$$\langle [v^i(t) - v^i(0)][v^j(t) - v^j(0)] \rangle \simeq \delta^{ij} C_0 \bar{\epsilon} t \quad (2)$$

with  $\bar{\epsilon}$  the mean viscous dissipation and  $C_0$  a universal constant; Eqn. (1) will then result from assuming a Markovian behaviour for  $\mathbf{v}$ , i.e. that  $a^i$  and  $\mathcal{B}^{ij}$  depend solely on the current values of  $\mathbf{v}$  and  $\mathbf{x}$  and not on their previous history.

The well-mixedness condition, introduced in [4], lead to a great advance in Lagrangian models, providing a simple technique for expressing the drift coefficient  $\mathbf{a}$  in Eqn. (1) in terms of observed properties of the flow. Some attention must be focused on how this approach works, because useful and simple results can be obtained only in some particular cases. For passive scalar transport, the application of the method is straightforward, and this is related to incompressibility of the flow.

In the current approach, it is assumed that the noise term  $d\mathbf{w}$  in Eqn. (1) accurately represents, in high Reynolds number turbulent regimes, the inertial range scaling of the Lagrangian velocity increments:

$$\mathcal{B}^{ij}(\mathbf{v}, \mathbf{x}, t) = \delta^{ij} C_0 \bar{\epsilon}(\mathbf{x}, t) \quad (3)$$

Then, the well-mixedness criterion allows us to determine the drift coefficient  $\mathbf{a}$  in terms of  $\bar{\epsilon}$  and the Eulerian Probability Density Function (PDF) for the fluid velocity  $\mathbf{u}(\mathbf{x}, t)$ :  $\rho_E(\mathbf{u}, t, \mathbf{x}) \equiv \rho(\mathbf{u}(\mathbf{x}, t))$ . These features make Lagrangian modelling the technique of choice in the case of the dispersion of pollutants in the ABL (atmospheric boundary layer).

The great advantage of the well-mixedness approach, coupled with Eqn. (3), is that no knowledge of the spatio-temporal structure of the turbulent fluctuations is required, rather, it is the outcome, encoded in the drift coefficient, of the well mixed condition. This strength of the model, however, turns into weakness, whenever the turbulent structure plays a relevant role. A first hint that this, actually, is always the case, is the non-uniqueness of the solution for  $\mathbf{a}$  given  $\bar{\epsilon}$  and  $\rho_E(\mathbf{u})$  [4, 6]. In the well mixedness approach, the drift coefficient  $\mathbf{a}$  is determined only up to a velocity curl, and interpretation of this "gauge" freedom in terms of the properties of the flow is awkward.

There are situations in which the structure of turbulence plays an explicit role. A first example is produced when coherent structures dominate the flow, a rather common occurrence in turbulence, which takes a dramatic form in near wall regions. These regions become relevant in many situations of practical interest in industrial flows, but also, to name a few, in the study of transport in tree canopies and in indoor pollution. These flows are often characterized by moderate Reynolds number, and, for this reason, not only the viscous scale may be not negligible, but a well developed inertial range may even be absent, so that the conditions justifying Eqn. (3) cease to be valid. Now, standard techniques exist which allow for the inclusion of non-Gaussianity [7] and anisotropy [8, 6] in Lagrangian models, as well as for the effect of finite Reynolds numbers [9]. However, these techniques do not take into account the geometric structure of the turbulent fluctuations, which calls for information about space correlation.

In the range of scales we are considering, another issue will come into play, if we are interested in modelling solid particle transport. In this case, non-tracer behaviours associated with inertia and gravity will begin to be felt (inertia and trajectory crossing effects [10, 11, 12]). This is especially true for atmospheric aerosol,

characterized by heavy particles with relative density of the order of 1000 and particle diameters in the range  $10^{-2} \div 10^2 \mu\text{m}$ . Inertia effects are generally negligible in ABL mesoscale modeling, but can become relevant in the near wall regions of wall bounded flows [13], which is relevant for problems of air conditioning and abatement of indoor pollution. Trajectory crossing effects related to gravity can have deep implications not only in wall bounded flows, but also for particulate transport in the ABL [10].

These effects reflect heavily on the possibility of using Eqns. (2-3) to model the Lagrangian velocity increments, and call back for the need of information on the spatio-temporal structure of the turbulent fluctuations.

Some attempts in this direction were carried on in [14, 15], but disregard of correlations between fluid velocity increments along solid particle trajectories lead to difficulties in the fluid particle limit [16] and in the implementation of the well-mixedness condition.

In order to be able to understand the constraints imposed by the turbulent structure on the form of a Lagrangian model, one may try a derivation from a velocity field  $\mathbf{u}(\mathbf{x}, t)$  of prescribed statistics. If the structure function  $\langle [u^i(\mathbf{x}, t) - u^i(0, 0)][u^j(\mathbf{x}, t) - u^j(0, 0)] \rangle$  scaled linearly for small space-time separations, the velocity increment between two points lying on a trajectory would be given by:

$$d\mathbf{u} = \langle [\partial_t + \mathbf{u}(x, t) \cdot \nabla] \mathbf{u}(\mathbf{x}, t) | \mathbf{u}(\mathbf{x}, t) \rangle dt + d\mathbf{w} \quad (4)$$

with  $\langle d\mathbf{w} \rangle = 0$  and  $d\mathbf{w}^2 = O(dt)$ . We could then introduce a Lagrangian model obeying Eqn. (1), with

$$\begin{cases} \mathbf{a}(\mathbf{v}, \mathbf{x}, t) = \langle [\partial_t + \mathbf{u}(x, t) \cdot \nabla] \mathbf{u}(\mathbf{x}, t) | \mathbf{u}(\mathbf{x}, t) = \mathbf{v} \rangle \\ \mathcal{B}^{ij}(\mathbf{v}, \mathbf{x}, t) dt = \langle dw^i dw^j | \mathbf{u}(\mathbf{x}, t) = \mathbf{v} \rangle \end{cases} \quad (5)$$

With the coefficients given in this equation, Eqn. (1) would provide a Markovianized version of the dynamics of a particle moving in the random velocity field  $\mathbf{u}(\mathbf{x}, t)$ .

It turns out that, provided the structure functions for  $\mathbf{u}$  scale linearly, the well-mixedness technique could be imposed directly on the random field  $\mathbf{u}(\mathbf{x}, t)$ , before any trajectory is defined. This means expressing the form of the conditional averages of the velocity derivatives:  $\langle \partial_t \mathbf{u}(\mathbf{x}, t) | \mathbf{u}(\mathbf{x}, t) \rangle$  and  $\langle \nabla \mathbf{u}(\mathbf{x}, t) | \mathbf{u}(\mathbf{x}, t) \rangle$  in terms of the

Eulerian PDF  $\rho_E(\mathbf{u}, \mathbf{x}, t)$ . Our result is that, if the flow is incompressible, a passive tracer flow will satisfy the ergodic property

$$\rho_L(\mathbf{v}|\mathbf{x}, t) = \rho_E(\mathbf{v}, \mathbf{x}, t) \quad (6)$$

where  $\rho_L(\mathbf{v}|\mathbf{x}, t)$  is the Lagrangian PDF for a tracer passing at the point  $\mathbf{x}$  at time  $t$ , to have velocity  $\mathbf{v}$ . In other words the well-mixedness condition imposed on the random field extends exactly to the Lagrangian model defined by Eqns. (1) and (5).

Clearly, linear scaling at small separations does not correspond to the properties of a real turbulent field, which, at high Reynolds numbers is more rough, and whose time correlations, due to the sweep effect, have Lagrangian nature at short time scales [5]. This is compensated, however, by control over the large scale structure of the correlations, which is the relevant aspect for the determination of turbulent transport.

A related issue, concerning solid particle transport, is that anomalous scaling of the fluid velocity increments sampled by a solid particle, are known to occur at sufficiently short time scales [17]. Analysis of the different ranges characterizing solid particle motion was carried on in [16], and Lagrangian models resolving the anomalous scaling range were presented in [18] and [16], based respectively on the use of fractional Brownian motion and synthetic turbulence algorithms. Again, consideration of these short-time effects is neglected in favour of control of large scale geometry.

Compared to the standard approach in Lagrangian modelling, the one proposed here has definite advantages. Spatio-temporal turbulent structures can be included in a relatively simple way (an example will be given in Section X regarding wall bounded flows). The non-uniqueness ("gauge fixing") problem is solved in a simpler way, since only purely Eulerian properties of the flow are invoked (helicity is one example). The advection of passive tracers and solid particles are treated exactly on the same footing, hence, extension of the model to solid particle transport is automatic and does not need introducing additional assumptions.

This paper is organized as follows. In section II, a local characterization of a random velocity field will be given, introducing generalized "four-dimensional" Langevin

and Fokker-Planck equations, and providing local and global existence conditions. The condition of local existence appears to take the form of a generalized form of the well-mixedness condition, which will be discussed in section III. This will be used to calculate conditional averages in the form  $\langle \nabla \mathbf{u} | \mathbf{u} \rangle$  and  $\langle \partial_t \mathbf{u} | \mathbf{u} \rangle$  from the property of  $d\mathbf{w}$  and the Eulerian velocity PDF, and the relation with the spatio-temporal structure of the random field will be discussed. In section IV, expressions for the noise amplitude  $\langle d\mathbf{w}d\mathbf{w} \rangle$  will be derived, and their relation with the symmetric sector of the velocity correlation will be discussed in terms of the SO(3) technique introduced in [19]. The antisymmetric sector of the velocity correlation will be discussed in section V, illustrating how it relates to the problem of non-uniqueness in the well-mixedness approach, and showing how helicity and other geometrical features could be included in the random field. Section VI will be devoted to the derivation of a Markovian Lagrangian model in the form of Eqn. (5), and to presentation of its main properties. Sections VII and VIII will be devoted to analysis of the Markovian approximation in the Lagrangian model and to proof of the ergodic property given by Eqn. (6). Sections IX and X will illustrate two applications of the Lagrangian model to solid particle transport, respectively, in homogeneous isotropic turbulence, and in a turbulent channel flow. Section XI contains the conclusions.

## II. Characterization of the random velocity field

Let us introduce a zero-mean, incompressible random velocity field  $\mathbf{u}(\mathbf{x}, t)$ , with 2nd order structure functions scaling linearly in the increment at small space-time separations. We introduce 4-vector notation:

$$x^\mu = \{x^0, x^i\} \equiv \{t, \mathbf{x}\}, \quad \partial_\mu \equiv \frac{\partial}{\partial x^\mu}. \quad (7)$$

and stick rigorously to the Einstein convention of summation over covariant-contravariant repeated indices. We have the following equation for the velocity increment:

$$du^i \equiv dx^\mu \partial_\mu u^i = A_\mu^i(\mathbf{u}, x^\mu) dx^\mu + dw^i \quad (8)$$

where

$$A_\mu^i(\mathbf{u}, x^\mu) = \langle \partial_\mu u^i(\mathbf{x}, t) | \mathbf{u}(\mathbf{x}, t) \rangle \quad (9)$$

and  $\langle d\mathbf{w} | \mathbf{u} \rangle = 0$ . From linearity, the contribution to the velocity structure function is dominated, for small values of the increments, by the correlation for  $d\mathbf{w}$ , and we have:

$$\langle dw^i dw^j | \mathbf{u}(\mathbf{x}, t) \rangle = \langle du^i(\mathbf{x}, t) du^j(\mathbf{x}, t) \rangle = O(|d\mathbf{x}|, dt) \quad (10)$$

We limit our analysis to random velocity fields where the statistics of the velocity increments is independent of that of the total velocity:

$$\langle dw^i dw^j | \mathbf{u} \rangle = \langle dw^i dw^j \rangle. \quad (11)$$

Incompressibility of the velocity field  $\partial_i u^i = 0$ , leads to the constraints:

$$A_i^i = 0, \quad \frac{\partial \langle \Delta w^i \Delta w^j \rangle}{\partial \Delta x^i} = 0 \quad (12)$$

From Eqns. (8) and (10), we obtain the following generalized Itô's Lemma; for a generic smooth function  $\phi(\mathbf{u})$ :

$$d\phi(\mathbf{u}) = (A_\mu^i dx^\mu + dw^i) \partial_{u^i} \phi(\mathbf{u}) + \frac{1}{2} \langle dw^i dw^j \rangle \partial_{u^i} \partial_{u^j} \phi(\mathbf{u}) \quad (13)$$

and from here, we can derive an equation for the change of the 1-point PDF  $\rho_E(\mathbf{u}, x^\mu) \equiv \rho(\mathbf{u}(\mathbf{x}, t))$ , in passing from the point  $x^\mu$  to to the point  $x^\mu + dx^\mu$ :

$$d\rho_E \equiv dx^\mu \partial_\mu \rho_E = -\partial_{u^i} (A_\mu^i dx^\mu \rho_E) + \frac{1}{2} \partial_{u^i} \partial_{u^j} (\langle dw^i dw^j \rangle \rho_E) \quad (14)$$

The sequence leading from Eqn. (8) to (14) is very suggestive, in that it generalizes the one from a Langevin to a Fokker-Planck equation [20]. However, contrary to the case of a standard Fokker-Planck equation, Eqn. (14) does not admit in general solution for  $\rho_E$ . In fact, once the noise amplitude  $\langle dw^i dw^j \rangle$  and the drift  $A_\mu^i$  are given, Eqn. (14) becomes a system of four partial differential equations for the single PDF  $\rho_E$ , and this system is generally over-determined. In the next section, it will be shown how a generalized version of the well-mixedness condition is able to take care of this local existence problem.

The ill-posedness of the problem is reflected at the global level, in the fact that a local definition for the "noise" increment amplitude  $\langle dw^i dw^j \rangle$  is not sufficient to

define a realization for  $\mathbf{w}(\mathbf{x}, t)$ , and consequently for  $\mathbf{u}(\mathbf{x}, t)$ . This in contrast with the case of the standard Langevin equation. In fact, if we integrate Eqn. (8) along a closed curve in space-time, and consider uncorrelated increments  $d\mathbf{w}$  along the curve, we will obtain in general a non-zero total velocity increment in the closed loop. In other words, if we disregard these correlations for  $\mathbf{w}$ , the differential  $d\mathbf{u}$  entering Eqn. (8) will not in general be exact.

The question becomes at this point the existence of a random velocity field with local structure described by Eqn. (8). It turns out that such a velocity field can be constructed explicitly, although the construction described below is by no means unique.

Given a point  $x^\mu$  and a direction in space time defined by the versor  $r^\mu$  ( $r^\mu r_\mu = 1$ ), we can introduce the stochastic process  $\hat{u}^i(s) \equiv \hat{u}^i(x^\mu, r^\mu; s)$  obeying the Langevin equation:

$$\begin{cases} d\hat{u}^i(s) = r^\mu A_\mu^i(\hat{\mathbf{u}}, x^\mu) ds + d\hat{w}^i \\ \langle d\hat{w}^i d\hat{w}^j \rangle = \frac{d}{ds} \langle [u^i(x^\mu + r^\mu s) - u^i(x^\mu)][u^j(x^\mu + r^\mu s) - u^j(x^\mu)] \rangle \Big|_{s=0^+} ds \end{cases} \quad (15)$$

The correlation functions for the stochastic process  $\hat{\mathbf{u}}(s)$ , starting from the second order one  $C^{ij}(x^\mu, sr^\mu) = \langle \hat{u}^i(x^\mu, r^\mu; s) \hat{u}^j(x^\mu, r^\mu; 0) \rangle$ , will identify a random velocity field  $\mathbf{u}(x^\mu)$  whose local statistical properties are those imposed by Eqn. (8), and whose restriction to straight lines in space time will be, by construction, Markovian. As with the correlation time of the solution of a standard Langevin equation, the correlation length in the direction  $r^\mu$  will be encoded in the drift coefficient  $r^\mu A_\mu^i(\hat{\mathbf{u}}, x^\mu)$ . A random field realization is obtained, in the simpler Gaussian case, by first carrying on the principal orthogonal decomposition (POD) of  $C^{ij}(x^\mu, \Delta x^\mu)$ , and then random superposing, with the appropriate amplitudes, the resulting POD modes [21].

### III. Determination of the drift

The real meaning of Eqn. (14) is to provide a consistency condition for  $\langle dw^i dw^j \rangle$  and  $A_\mu^i$ , that could be used to generalize the Thomson-87 technique and determine from  $\langle dw^i dw^j \rangle$  and  $\rho_E$ , the expression for  $A_\mu^i$ . The difference with the standard case is

that, instead of calculating the conditional mean  $\langle \partial_t v^i | \mathbf{v} \rangle$  of the Lagrangian velocity time derivative, we seek here the conditional mean of all the derivatives of the Eulerian velocity, namely  $\langle \partial_\mu u^i | \mathbf{u} \rangle$ . These averages contain important information on the behaviour of the velocity correlation  $C^{ij}(x^\mu, \Delta x^\mu) = \langle u^i(x^\mu) u^j(x^\mu + \Delta x^\mu) \rangle$ :

$$C^{ij}(x^\mu, \Delta x^\mu) = \frac{1}{2}[R^{ij}(x^\mu) + R^{ij}(x^\mu + \Delta x^\mu)] - \frac{1}{2}\langle \Delta u^i \Delta u^j \rangle + C_A^{ij} \quad (16)$$

Here,  $R^{ij}(x^\mu) = C^{ij}(x^\mu, 0)$  indicates the Reynolds tensor, while

$$C_A^{ij} = \frac{1}{2}[C^{ij}(x^\mu, \Delta x^\mu) - C^{ij}(x^\mu + \Delta x^\mu, -\Delta x^\mu)] \quad (17)$$

is the antisymmetric part of the velocity correlation. It is clear that the noise amplitude is associated with the symmetric sector of the velocity correlation.

Let us try to generalize the Thomson-87 approach to calculate the drift  $A_\mu^i$  from  $\rho_E$ . It is convenient to split the drift into three pieces:

$$A_\mu^i = \bar{A}_\mu^i + \frac{1}{\rho_E} \Phi_\mu^i + \frac{1}{\rho_E} \Psi_\mu^i \quad (18)$$

where  $\bar{A}_\mu^i$  is chosen to cancel the noise term in the Fokker-Planck equation (14). Exploiting independence of the noise amplitude from  $\mathbf{u}$ :

$$\bar{A}_\mu^i dx^\mu = \frac{1}{2} \langle dw^i dw^j \rangle \partial_{u^j} \log \rho_E \quad (19)$$

and  $\bar{A}_\mu^i$ , from the second of Eqn. (12), is automatically traceless. The term  $\Phi_\mu^i$  is chosen to cancel the contributions to Eqn. (14) from statistical non-uniformity and non-stationarity:

$$\partial_{u^i} \Phi_\mu^i = -\partial_\mu \rho_E \quad (20)$$

The term  $\Psi$  is necessary to cancel the trace of  $\Phi$  and must be divergenceless with respect to  $\mathbf{u}$ :

$$\partial_{u^i} \Psi_j^i = 0, \quad \Psi_0^i = 0 \quad \Psi_i^i = -\Phi_i^i \quad (21)$$

As in the Thomson-87 approach [4], the drift is defined up to a gauge term  $\frac{1}{\rho_E} \Xi_\mu^i$  satisfying:

$$\Xi_i^i = 0, \quad \partial_{u^i} \Xi_\mu^i = 0 \quad (22)$$

which, substituted into Eqn. (14), will produce an identically zero contribution.

The drift  $A_\mu^i$  is associated with the velocity correlation through the equation:

$$\langle u^i \Delta u^j \rangle = \langle u^i \langle \Delta u^j | \mathbf{u} \rangle \rangle = \Delta x^\mu \langle u^i A_\mu^j \rangle, \quad (23)$$

Let us analyze individually each of the terms in  $A_\mu^i$ . Substituting Eqn. (19) into Eqn. (23) we see that  $\bar{A}_\mu^i$  gives just the symmetric piece of the correlation, i.e. the  $-\frac{1}{2}\langle \Delta u^i \Delta u^j \rangle$  in Eqn. (23). The  $\Phi$  and  $\Psi$  terms are more easily analyzed in Fourier space:  $\tilde{f}(\boldsymbol{\eta}) = \int d^3u e^{-i\boldsymbol{\eta}\cdot\mathbf{u}} f(\mathbf{u})$ . Using Eqns. (18-19), Eqn. (23) will read:

$$\langle u^i \Delta u^j \rangle = -\frac{1}{2}\langle \Delta w^i \Delta w^j \rangle - i\Delta x^\mu \partial_{\eta_j} (\tilde{\Phi}_\mu^i + \tilde{\Psi}_\mu^i)|_{\eta=0} \quad (24)$$

Using the fact that the generating function  $\tilde{\rho}_E$  obeys  $\tilde{\rho}_E = 1 - \frac{1}{2}R^{ij}\eta_i\eta_j + O(\eta^3)$ , we can write, from Eqn. (23):

$$\tilde{\Phi}_\mu^i = -\frac{i}{2}\partial_\mu R^{ij}\eta_j + O(\eta^2) \quad (25)$$

so that the contribution from  $\Phi$  to the correlation function is, from Eqn. (24):  $\frac{1}{2}dx^\mu \partial_\mu R^{ij}$ , which accounts for the spatial inhomogeneity of the correlation [the  $\frac{1}{2}(R^{ij} + R^{ji})$  term on RHS of Eqn. (16), which is centered at  $\sim x^\mu + \Delta x^\mu/2$ ].

We see that  $\bar{A}_\mu^i$  and  $\Phi_\mu^i$  account for all of the contribution to the correlations, which either are symmetric, or come from inhomogeneity of the statistics. We know at this point that both  $\Psi_\mu^i$  and  $\Xi_\mu^i$  will be able to contribute only to the antisymmetric part of  $A_\mu^i$ . We give in explicit form the contribution from  $\Psi_\mu^i$ . Exploiting the first of Eqn. (21), we utilize the ansatz:

$$\tilde{\Psi}_j^i = i(\delta_j^i \eta_k \tilde{\psi}^k - \eta_j \tilde{\psi}^i), \quad \tilde{\Psi}_0^i = 0 \quad (26)$$

and, from  $\Psi_i^i = -\Phi_i^i$  and Eqn. (25):

$$\tilde{\psi}^k = \frac{1}{4}(\partial_l R^{lk}) + \epsilon^{klm} \eta_l \tilde{f}_m + O(\eta^2) \quad (27)$$

with  $\mathbf{f}$  arbitrary. The contribution to  $\Psi_j^i$  from  $\mathbf{f}$  is traceless and can be reabsorbed into the gauge term  $\Xi$ ; the final result is therefore:

$$\tilde{\Psi}_j^i = \frac{i}{4}[\delta_j^i (\partial_l R^{lk}) \eta_k - (\partial_l R^{li}) \eta_j] + O(\eta^3) \quad (28)$$

and the contribution to the correlation function is:  $\frac{1}{4}[\partial_l R^{lk} dx^i - \partial_l R^{li} dx^k]$ , which is antisymmetric as required.

Explicit expressions for the drift terms are promptly obtained in the case of Gaussian statistics (expressions for the case of a symmetric  $\rho_E$  with kurtosis larger than three are given in the Appendix A). The velocity PDF reads therefore:

$$\rho_E(\mathbf{u}, x^\mu) \equiv \rho_G(\mathbf{u}, x^\mu) = (8\pi^3 ||R||)^{-\frac{1}{2}} \exp\left(-\frac{1}{2} S_{ij} u^i u^j\right) \quad (29)$$

with  $S_{ij} = (R^{-1})_{ij}$  the Reynolds tensor inverse. In this case, the higher order terms in  $\eta_i$  entering Eqns. (25-28) disappear and we are left with:

$$\bar{A}_\mu^i dx^\mu = -\frac{1}{2} \langle dw^i dw^j \rangle S_{jk} u^k \quad (30)$$

$$\Phi_\mu^i = \frac{1}{2} (\partial_\mu R^{ik}) S_{kl} u^l \rho_E \quad (31)$$

$$\Psi_j^i = \frac{1}{4} [-\delta_j^i (\partial_l R^{lk}) S_{km} + (\partial_l R^{li}) S_{jm}] u^m \rho_E \quad (32)$$

We can use these explicit expressions to obtain more informations on the nature of the various contributions to the drift. In analogy to the case of the standard Langevin equation, we see that  $\bar{A}_\mu^i$  must be discontinuous at  $\Delta x^\mu = 0$ . From Eqn. (19), discontinuity of the correlation function derivative at  $\Delta x^\mu = 0$  is necessary to balance the linear scaling of  $dw^2$ . In the coordinate system where, for the given  $\Delta x^\mu$ ,  $\bar{A}_j^i$  is diagonal, we shall then have:

$$\langle \Delta u^i | \mathbf{u} \rangle \sim -|\Delta x^i| \quad (33)$$

As regards  $\Phi_\mu^i$ , we see from Eqn. (31) that it produces an amplification of  $\mathbf{u}$  when  $dx^\mu$  is directed to a region in space-time where the turbulence is stronger (this is easy to see when  $R^{ij} \propto \delta^{ij}$ ).

Finally, the  $\Psi$  term, turns out to produce a complicated mixture of rotations and amplification of the velocity vector. Indicating  $\tilde{u}_i = S_{ik} u^k$ , and choosing the coordinate system so that  $\partial_i R^{il} = 4\tilde{c}\delta_1^l$ , and  $\Delta x^3 = 0$  we have from Eqn. (32):

$$\langle \Delta u^1 | \mathbf{u} \rangle = \tilde{c}\tilde{u}_2 \Delta x^2, \quad \langle \Delta u^2 | \mathbf{u} \rangle = -\tilde{c}\tilde{u}_1 \Delta x^2, \quad \langle \Delta u^3 | \mathbf{u} \rangle = 0. \quad (34)$$

If  $R^{ij} \propto \delta^{ij}$ , we will have  $\tilde{u}_i = u_i$  and the result of Eqn. (34) will be a rotation of  $\mathbf{u}$  in the plane 12 as one moves in the direction  $x_2$ .

## IV. Determination of the noise tensor

In order to obtain the drift coefficients, which give the decay of the turbulent correlations in the various space-time directions, it is necessary first to determine the form of the noise tensor  $\langle dw^i dw^j \rangle$ . In fact, it is in the noise that all the information on the turbulent structure is encoded (at least that part relative to the symmetric sector of the correlations).

A very general form for the noise tensor, satisfying the incompressibility condition  $\partial \langle \Delta w^i \Delta w^j \rangle / \partial x^i = 0$ , is a superposition of terms in the form (here and in the rest of this section, we shall identify space-time increments with  $x^\mu$ ,  $\mathbf{x}$  and  $t$ , while the dependence on the space-time position is left unindicated):

$$\langle \Delta w^i \Delta w^j \rangle = \frac{2u_T^2}{\tau_E} [B_t^{ij}(t) + B^{ij}(\mathbf{x} - \bar{\mathbf{u}}t)]; \quad \partial_i B^{ij}(\mathbf{x}) = 0 \quad (35)$$

where  $u_T^2 = \frac{1}{3}R_i^i$ ,  $\tau_E$  has the meaning of an Eulerian correlation time and  $B_t^{ij} = |t|\delta^{ij} + \hat{B}_t^{ij}$ , with  $\hat{B}_t^{ij}$  symmetric and traceless.

We see that the presence of mixed space-time increment contributions can account for situations in which the time correlations have Lagrangian nature. In this way, pure time decorrelation will take place in the reference system moving locally with the mean flow  $\bar{\mathbf{u}}$ . A situation with purely Eulerian time correlation will be realized by putting  $\bar{\mathbf{u}} = 0$ .

It is to be noticed that the simplified form of space-time mixing allowed for by Eqn. (35) corresponds to a situation in which all space scales decay with identical characteristic time. If the dependence of the decay time  $\tau(x)$  on the space scale  $x$  were taken into account (which would impose in our case  $\tau(x) \sim x$ ), we would find that the sweep and the time decay of fluctuations contribute equally to velocity decorrelation along a Lagrangian trajectory, signaling crossover to a sweep dominated regime for sublinear scaling of the second order space structure function. Being interested in the structure of the noise as given by Eqn. (35), only as a tool to construct the large scale features of the random field, we shall not pursue these issues further.

In moderately anisotropic situations, it may be expedient to expand the space component  $B^{ij}$  in spherical tensors, following the SO(3) decomposition technique

[19]. Due to the symmetry of  $\langle \Delta w^i \Delta w^j \rangle$ , only even harmonics are present and we write:

$$B^{ij}(\mathbf{x}) = \sum_{n=0} B_{2n}^{ij}(\mathbf{x}) \quad (36)$$

where  $B_l^{ij}$  is a combination of  $l$ -th order spherical tensors (see Appendix B). To keep the lowest order anisotropic contribution, we consider up to  $l = 2$ . The incompressibility condition  $\partial_i(B_l^{ij})$  gives then (the hats identify versors):

$$B^{ij}(\mathbf{x}) = \frac{|\mathbf{x}|}{u_T} \left[ (a + 4b^{lm} \hat{x}_l \hat{x}_m) \delta^{ij} + \frac{1}{3} (-a + (2b^{lm} - c^{lm}) \hat{x}_l \hat{x}_m) \hat{x}^i \hat{x}^j - \hat{x}_l [(2b^{li} + c^{li}) \hat{x}^j + (2b^{lj} + c^{lj}) \hat{x}^i] + 4c^{ij} \right] \quad (37)$$

where  $a$  gives the  $l = 0$  part, while the tensors  $b^{ij}$  and  $c^{ij}$ , which are symmetric and traceless, account for the the  $l = 2$  part. We consider next some relevant limit cases.

#### *Isotropic turbulence*

In this case, all the spherical tensors with  $l > 0$  are zero. We are thus left with the simple expression:

$$\langle \Delta w^i \Delta w^j \rangle = \frac{2u_T^2}{\tau_E} \left[ |t| \delta^{ij} + \frac{a|\mathbf{x}|}{u_T} \left( \delta^{ij} - \frac{1}{3} \hat{x}^i \hat{x}^j \right) \right] \quad (38)$$

The parameter  $a$  identifies a length-scale  $l_u = u_T \tau_E / a$  for the fluctuations and has therefore the meaning of a ratio between the eddy life-time  $\tau_E$  and the eddy rotation time  $l_u / u_T$ .

#### *Long axisymmetric vortices*

Let us imagine that the correlation tensor is dominated by the effect of long axisymmetric vortices directed along  $x^1$ . Let us try to use this information to impose a structure to the space structure tensor  $B^{ij}$  defined in Eqn. (37). Let us impose the condition that  $B^{ij}(\mathbf{x}) = 0$  for  $\mathbf{x} = \{x, 0, 0\}$ . For  $\mathbf{x} = \{x, 0, 0\}$ , we have from Eqn. (37):

$$\frac{u_T B^{11}}{|\mathbf{x}|} = \frac{1}{3} (2a + 2b^{11} + 5c^{11}), \quad \frac{u_T B^{22}}{|\mathbf{x}|} = a + 4b^{11} + 4c^{22}, \quad \frac{u_T B^{33}}{|\mathbf{x}|} = a + 4b^{11} + 4c^{33},$$

$$\frac{u_T B^{12}}{|\mathbf{x}|} = 3c^{12} - 2b^{12}, \quad \frac{u_T B^{13}}{|\mathbf{x}|} = 3c^{13} - 2b^{13}, \quad \frac{u_T B^{23}}{|\mathbf{x}|} = 4c^{23}. \quad (39)$$

and we find immediately the result:

$$c^{12} = c^{13} = \frac{2}{3}b^{12} = \frac{2}{3}b^{13}; \quad c^{23} = 0;$$

$$b^{11} = -\frac{3}{8}a; \quad b^{22} = b^{33} = \frac{3}{16}a; \quad c^{11} = -\frac{a}{4}; \quad c^{22} = c^{33} = \frac{a}{8}. \quad (40)$$

We are free to impose the condition  $b^{ii} = c^{ii} = 0$  for  $i \neq 1$  and we reach the expression for generic  $\mathbf{x}$  of the  $B$  components along 11 and 22:

$$\begin{cases} \frac{u_T B^{11}(\mathbf{x})}{|\mathbf{x}|} = \frac{1}{6}\hat{x}_1^2 + \frac{3}{4}\hat{x}_\perp^2 - \frac{1}{6}\hat{x}_1^4 + \frac{1}{12}\hat{x}_1^2\hat{x}_\perp^2 \\ \frac{u_T B^{22}(\mathbf{x})}{|\mathbf{x}|} = \frac{3}{2} - \frac{3}{2}\hat{x}_1^2 + \frac{3}{4}\hat{x}_\perp^2 - \frac{4}{3}\hat{x}_2^2 - \frac{1}{6}\hat{x}_1^2\hat{x}_2^2 + \frac{1}{12}\hat{x}_\perp^2\hat{x}_2^2 \end{cases} \quad (41)$$

where  $x_\perp^2 = x_2^2 + x_3^2$ . Analyzing Eqn. (41) in function of  $\hat{x}_1$  first for  $\hat{x}_2 = 0$  and then for  $\hat{x}_2 = \hat{x}_\perp$ , it is possible to show that  $B^{ij}$  is always positive defined, as required.

### *Two-dimensional structures*

Suppose that the flow is 2-dimensional, say  $\mathbf{u} = \{u_1, 0, u_3\}$ . In this case, the SO(3) decomposition reduces to an SO(2) one. Keeping again only the lowest order anisotropic correction, we find, for  $\mathbf{x} = \{x_1, 0, x_3\}$ :

$$\begin{aligned} B^{ij}(\mathbf{x}) = \frac{|\mathbf{x}|}{u_T} & [(a + 3b^{lm}\hat{x}_l\hat{x}_m)\delta^{ij} + \frac{1}{2}(-a + (b^{lm} - c^{lm})\hat{x}_l\hat{x}_m)\hat{x}^i\hat{x}^j \\ & - \hat{x}_l[(2b^{li} + c^{li})\hat{x}^j + (2b^{lj} + c^{lj})\hat{x}^i] + 3c^{ij}] \end{aligned} \quad (42)$$

where  $b^{22} = b^{33} = 0$  and the traceless condition imposes  $b^{33} = -b^{11}$ ,  $c^{33} = -c^{11}$ .

### *Streaks*

Contrary to the three-dimensional case, elongated structures cannot be accommodated in the SO(2) decomposition: the resulting noise tensor would not be positive definite. Two-dimensional streaks along the direction of the mean flow appear to be one of the characteristic structures in the viscous sublayer of wall turbulence

[5]. If the streaks are oriented along  $x_1$ , and again, the flow is two-dimensional in the  $x_1x_3$  plane, the noise tensor will take the form

$$B^{ij}(\mathbf{x}) = a \frac{|x_3|}{u_T} \delta_1^i \delta_1^j \quad (43)$$

In the Gaussian case, Eqns. (8) and (30) lead to exponential decay for the correlation at large separations. Following Eqn. (15), this means correlation lengths in the direction  $r^\mu$  given by the inverse of  $\langle u^i r^\mu \bar{A}_\mu^j \rangle$ . These correlations will be calculated explicitly in section VIII.

If the statistics is non Gaussian and is modelled by a bi-Gaussian distribution [7, 22, 23], as described in Eqn. (A1), this direct correspondence between the tensor  $\bar{A}_\mu^i$  and the correlation lengths of the field will not be present anymore. A double exponential decay of correlations ensues, with the slower decay associated with the intermittent bursts (see Appendix A) [24]. In consequence of this, to have the desired space and time scales for the bursts, it is necessary to renormalize the noise amplitude, with respect to the Gaussian case, by the factor  $\beta = (2/3)k - 1$  with  $k$  the kurtosis [see Eqn. (A2)].

## V. Gauge fixing and the antisymmetric sector

Once the noise tensor and the PDF  $\rho_E$  are fixed and the well-mixedness condition is imposed, the symmetric sector of the velocity correlation is completely determined. The gauge term  $\Xi_\mu^i$  can be used to fix the structure of the anisotropic sector. We consider for simplicity the homogeneous case  $C^{ij}(x^\mu, \Delta x^\mu) = C^{ij}(\Delta x^\mu)$ .

We discover immediately the following important fact: not all expressions for the gauge term  $\Xi_\mu^i$ , and consequently for  $A_\mu^i$ , lead to a statistically realizable  $C^{ij}(\Delta x^\mu)$ . This is a different face of the problem of local existence for the solutions of Eqn. (14). Consider as a first example:  $\Xi_j^i = \epsilon^{i2}_j u^2$ . A contribution  $\Delta C^{11} = \epsilon^{12}_3 R^{12} dx^3$  is then added to  $C^{11}(d\mathbf{x})$ , with  $d\mathbf{x} = \{0, 0, dx^3\}$ , that has the inadmissible symmetry  $\Delta C^{ij}(d\mathbf{x}) = -\Delta C^{ji}(-d\mathbf{x})$ . The second example is  $\Xi_0^1 = u^2$ ,  $\Xi_0^2 = -u^1$ ; in this case we find a contribution  $R^{12} dt$  to  $C^{12}(dt)$  with the inadmissible symmetry  $\Delta C^{12}(dt) = -\Delta C^{21}(dt)$ .

We seek a form of  $\Xi_\mu^i$  satisfying all the required symmetries, but still sufficiently general to describe most geometric structures one may think of. Let us start then by introducing the Gaussian PDF  $\rho_G$  whose second moments (i.e. the components of the Reynolds tensor) coincide with those of the Eulerian PDF  $\rho_E$  [see Eqn. (29)]. It is easy to see that the following expression for  $\Xi$  satisfies the divergence free condition  $\partial_{u^i}\Xi_\mu^i$  [the second of Eqn. (22)]:

$$\Xi_\mu^i = \rho_G \xi_\mu^l \epsilon_{lmj} R^{mj} u^j \quad (44)$$

where  $\xi_\mu^l$  does not depend on  $\mathbf{u}$ . The resulting contribution to the correlation function is:

$$\langle u^k \Delta u^i \rangle_\Xi = \Delta x^\mu \xi_\mu^l \epsilon_{lmj} R^{mj} R^{kj} \quad (45)$$

and the antisymmetry condition  $\langle u^k \Delta u^i \rangle_\Xi = -\langle u^i \Delta u^k \rangle_\Xi$  as well as the more general condition  $C^{ij}(x^\mu, \Delta x^\mu) = C^{ji}(x^\mu + \Delta x^\mu, -\Delta x^\mu)$  are both verified. Notice that if a bi-Gaussian is used to model  $\rho_E$ , the ratio  $\rho_G/\rho_E$  will decay like a Gaussian for large  $u$ , when the slowly decaying Gaussian entering  $\rho_E$ , which decays slower than  $\rho_G$  as well [see Eqns. (A1), (A2) and (A4)] becomes dominant.

To impose zero trace on the space components [first one of Eqn. (22)], it is convenient to separate the antisymmetric part of  $\xi_\mu^l$ :

$$\xi_m^l = \bar{\xi}_m^l + \epsilon^l_{mk} \zeta^k \quad (46)$$

The zero trace condition becomes:

$$\Xi_i^i = \rho_G \{ \bar{\xi}_i^k R^{im} \epsilon_{klm} u^l + [R_i^i \zeta_l - R_l^i \zeta_i] u^l \} = 0 \quad (47)$$

which must be satisfied for any  $u^l$ . This leads to the relation between  $\zeta^k$  and  $\bar{\xi}_m^l$ :

$$(R_l^j - R_k^k \delta_l^j) \zeta_j = \frac{1}{2} \epsilon_{klm} [\bar{\xi}^k C - C \bar{\xi}]^{km} \quad (48)$$

The presence of the commutator  $[\bar{\xi}^k C - C \bar{\xi}]^{km}$  suggests that we should work in the diagonal system for  $R^{ij}$ . It becomes easy in this way to separate the part of  $\bar{\xi}_j^i$  which anticommutes with  $R^{ij}$ , which is simply the part out of diagonal. Solution of Eqn. (48) gives then in the diagonal coordinate system, after little algebra:

$$\zeta_1 = \bar{\xi}_{23} \frac{R_{22} - R_{33}}{R_{22} + R_{33}}, \quad \zeta_2 = \bar{\xi}_{13} \frac{R_{33} - R_{11}}{R_{11} + R_{33}}, \quad \zeta_3 = \bar{\xi}_{12} \frac{R_{11} - R_{22}}{R_{11} + R_{22}}. \quad (49)$$

We are now in the position to determine the effect of the various components of  $\Xi_i^j$ , on  $A_i^j$  and on the velocity correlations.

*Time component*

It turns out that the  $\mu = 0$  component of Eqn. (44) is associated with a combination of rotation and strain of the velocity, as time passes, at any given position  $\mathbf{x}$ ; this is the Eulerian version of the mean velocity rotation along Lagrangian trajectories discussed in [6]. Working in the diagonal coordinate system for  $R^{ij}$ , the contribution from  $\xi^3_0$  will be, for instance:

$$\Xi_0^1 = \rho_G \xi^3_0 R^{11} u^2, \quad \Xi_0^2 = -\rho_G \xi^3_0 R^{22} u^1 \quad (50)$$

This turns into a pure rotation if  $R^{ij} \propto \delta^{ij}$ .

*Space component: diagonal part*

Also this component is associated with a combination of rotation and strain of the velocity, this time, as one moves at fixed time from one space point to another. Focusing e.g. on the contribution from  $\bar{\xi}_2^2$ , we find in the diagonal system for  $R^{ij}$ :

$$\Xi_2^1 = -\rho_G \bar{\xi}_2^2 R^{11} u^3, \quad \Xi_2^3 = \rho_G \bar{\xi}_2^2 R^{33} u^1 \quad (51)$$

In the case  $R^{ij} \propto \delta^{ij}$ , this becomes a pure rotation in the plane  $x^1 x^3$  as one moves in the  $x^2$  direction. The diagonal component of the spatial gauge term is the one associated with the presence of helicity  $H$  in the turbulent field. Indicating with  $\omega^i = \epsilon^{ij}_k \partial_j u^k$  the vorticity, we can write

$$H = \langle u_i \omega^i \rangle = \langle u_i \langle \omega^i | \mathbf{u} \rangle \rangle = \epsilon^{ij}_k \langle u_i A_j^k \rangle. \quad (52)$$

Substituting the various contributions to  $A_j^k$  in the above formula, we see that the only terms giving non-zero result are the diagonal ones in  $\bar{\xi}$ . Working in the diagonal coordinate system, we obtain then:

$$H = 2[\bar{\xi}_{11} R_{22} R_{33} + \bar{\xi}_{22} R_{11} R_{33} + \bar{\xi}_{33} R_{11} R_{22}] \quad (53)$$

*Space component: part out of diagonal*

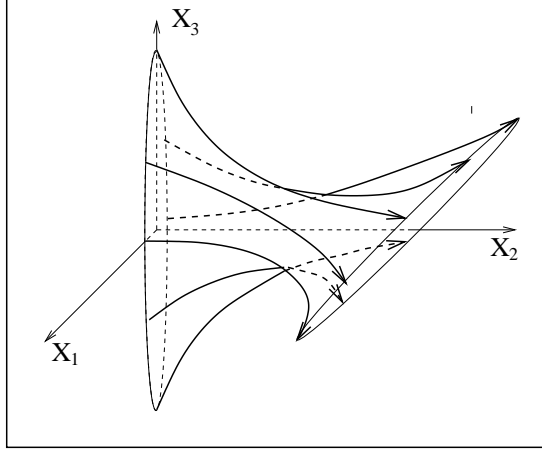


Figure 1: Sketch of the velocity lines in a coherent structure characterized by a non-zero value of  $\bar{\xi}_1^3$  (part out of diagonal of the spatial gauge term). The velocity components in the 13 plane are arranged along strain line with expanding and compressing directions respectively along  $x_1$  and  $x_3$ .

The effect of this component is illustrated, for the contribution from  $\bar{\xi}_1^3$ , in Figure 1. This effect consists of a strain of the velocity components as one moves in the direction 2. We give in the equation below the non-zero matrix elements of  $\Xi_k^i$  corresponding to  $\bar{\xi}_1^3$  (components still evaluated in the diagonal coordinate system).

$$\begin{cases} \Xi_1^1 = 2\rho_G \bar{\xi}_1^3 \frac{R_{11}R_{33}}{R_{11}+R_{33}} u_2, & \Xi_1^2 = -\rho_G \bar{\xi}_1^3 R_{22} u_1, \\ \Xi_2^1 = 2\rho_G \bar{\xi}_1^3 \frac{R_{11}(R_{11}-R_{33})}{R_{11}+R_{33}} u_1, & \Xi_2^3 = 2\rho_G \bar{\xi}_1^3 \frac{R_{33}(R_{11}-R_{33})}{R_{11}+R_{33}} u_3, \\ \Xi_3^2 = \rho_G \bar{\xi}_1^3 R_{22} u_3, & \Xi_3^3 = -2\rho_G \bar{\xi}_1^3 \frac{R_{11}R_{33}}{R_{11}+R_{33}} u_2. \end{cases} \quad (54)$$

## VI. Derivation of a Markovian Lagrangian model

Knowing the form of the tensors  $A_\mu^i$  and  $\langle dw^i dw^j \rangle$ , allows us to derive a Lagrangian stochastic model. This is done most naturally setting in Eqn. (8)  $dx^\mu = \{dt, \mathbf{v}dt\}$ , where  $\mathbf{v}$  is the particle velocity. Now, this entails a Markovian assumption on the Lagrangian statistics, whose validity will be checked in the next two sections, although it is not very different from the one used in standard Lagrangian models.

Let us write explicitly the Langevin and Fokker-Planck equations associated with our Lagrangian model, considering first the simpler case of a passive tracer  $dx^\mu = \{dt, \mathbf{u}dt\}$  where  $\mathbf{u}(t)$  identifies the fluid velocity sampled by the moving

particle:

$$du^i \equiv \dot{u}^i dt = (\mathbf{u} \cdot \mathbf{A}^i + A_0^i) dt + dw^i \quad (55)$$

$$(\partial_t + \mathbf{u} \cdot \nabla) \rho_L + \partial_{u^i} [(\mathbf{u} \cdot \mathbf{A}^i + A_0^i) \rho_L] = \frac{1}{2} \partial_{u^i} \partial_{u^j} (\mathcal{B}^{ij} \rho_L) \quad (56)$$

where  $\mathcal{B}^{ij} = \frac{d}{d\Delta t} \langle \Delta w^i \Delta w^j \rangle = \frac{u_T^2}{\tau_E} [B_t^{ij}(1) + B^{ij}(\mathbf{u})]$  [see Eqn. (35)].

In the Gaussian case, the drift term  $\mathbf{u} \cdot \mathbf{A}^i + A_0^i$  is in the quadratic form discussed in [4]. The incompressibility condition of Eqn. (12) and the consequent form of the terms  $\Phi$  and  $\Psi$  given by Eqns. (31-32) fix the choice of quadratic model in unique way (the resulting choice does not coincide with the one by Thomson [4], but is included in the set of possible solutions described in [6]).

As regards the noise term, we started in section II with an additive noise and we have arrived here at a multiplicative noise term (which is automatically intended, in the approach that we have followed, in the Itô sense [20]). This is obvious consequence of the fact that the amplitude  $\mathcal{B}^{ij}$  is conditioned to the increment being taken along the direction of motion of a fluid element. This dependence on  $\mathbf{u}$  disappears if we take the Kraichnan model limit [25] of  $\tau_E$  much shorter than the eddy rotation time, i.e.  $a \rightarrow 0$  [see comments after Eqn. (38)], which corresponds to the diffusive limit  $C_0 \rightarrow \infty$  in standard Lagrangian models [4]. The way in which this limit is carried out is different in the two approaches: in ours, it is the turbulence integral scale  $l_u$  that is sent to infinity [see comment after Eqn. (38)]; in the standard approach, the  $C_0 \rightarrow \infty$  limit corresponds directly to the one  $\tau_E \rightarrow 0$ .

For this reason, establishing a correspondence between the  $a \rightarrow 0$  limit in our model and standard Lagrangian models [for which the noise amplitude is given by Eqn. (3)] is not possible for physical values of the constant  $C_0$ .

The physical value of the model described by Eqns. (55-56) lies in the following result: for an incompressible  $\mathbf{u}(\mathbf{x}, t)$ , the uniform concentration solution to Eqn. (56) coincides with  $\rho_E$ ; in other words, the ergodic property is satisfied. (More precisely, independently on any Markovian approximation, the velocity PDF sampled by a passive tracer advected by the random field coincides with the Eulerian PDF  $\rho_E$ ). The proof of this result will be given in the next section. The well mixedness condition introduced in Section III takes therefore its standard meaning of a tool to

fix the form of the drift term in the Lagrangian model described by Eqns. (55-56).

Notice that, in its more general form, the well-mixedness condition is essentially an inverse problem: given an assigned Lagrangian PDF  $\rho_L(\mathbf{u}, \mathbf{x}, t)$ , the drift coefficients  $\mathbf{u} \cdot \mathbf{A}^i + A_0^i$  and the noise terms  $\mathcal{B}^{ij}$  entering Eqn. (56) can be related one to another by imposing  $\rho_L$  to be solution of the associated Fokker-Planck equation. In the case of an incompressible flow, the solution of Eqn. (56) starting from an initial uniform concentration profile coincides with  $\rho_L(\mathbf{u}|\mathbf{x}, t)$ , and can be chosen as the assigned PDF  $\rho_L$  from which  $\mathbf{u} \cdot \mathbf{A}^i + A_0^i$  is determined. Ergodicity guarantees at this point that  $\rho_L(\mathbf{u}|\mathbf{x}, t) = \rho_E(\mathbf{u}, \mathbf{x}, t)$ , the last PDF being directly measurable.

We do not expect the ergodic property to hold for solid particles, since the suspended phase flow, due to inertia, is now compressible, and preferential concentration phenomena are known to occur [26]. This means that it is not possible to impose a well-mixedness condition on the Lagrangian PDF, which now is not related any more to  $\rho_E$ . Nonetheless, the well-mixedness condition remains valid at the random field level. We can therefore derive, exactly as in the passive scalar case, a Lagrangian model. The solid particle dynamics obeys an equation, which in quite general form (neglecting memory effects associated with the Basset force) can be written as:

$$\dot{\mathbf{v}} = \mathbf{F}(\mathbf{v}, \mathbf{u}) \quad (57)$$

A general form was derived by [27], who neglect lift effects [28]. These equations are all derived in the limit of particle diameter  $d$  small with respect to the scales of the flow, and low particle Reynolds number  $Re_p = d|\mathbf{u} - \mathbf{v}|/\nu$ , where  $\nu$  is the kinematic viscosity. We will consider Eqn. (57) in simplified form by accounting only for linear Stokes drag and gravity:

$$\dot{\mathbf{v}} = \frac{\mathbf{u} - \mathbf{v} + \mathbf{v}_G}{\tau_S} \quad (58)$$

where  $\tau_S = 1/18 \gamma d^2/\nu$ , with  $\gamma$  the density of the particle relative to that of the fluid, is the Stokes time, and  $\mathbf{v}_G$  is the particle terminal velocity in a uniform force field. In the case of gravity:  $\mathbf{v}_G = \tau_S \mathbf{g}$  with  $\mathbf{g}$  the gravitational acceleration.

The analogue of Eqn. (55), in the solid particle case will now read:

$$du^i \equiv \dot{u}^i dt = (\mathbf{v} \cdot \mathbf{A}^i + A_0^i) dt + dw^i \quad (59)$$

where now  $\mathbf{u}(t)$  is the fluid velocity sampled by the solid particle moving with velocity  $\mathbf{v}(t)$ . The Lagrangian PDF  $\rho_L(\mathbf{u}, \mathbf{v}, \mathbf{x}, t)$  will obey the Fokker-Planck equation:

$$(\partial_t + \mathbf{v} \cdot \nabla)\rho_L + \partial_{v^i}(F^i \rho_L) + \partial_{u^i}[(\mathbf{v} \cdot \mathbf{A}^i + A_0^i)\rho_L] = \frac{1}{2}\partial_{u^i}\partial_{u^j}(\mathcal{B}^{ij}\rho_L) \quad (60)$$

where now  $\mathcal{B}^{ij} = \frac{u_i^2}{\tau_E}[B_t^{ij}(1) + B^{ij}(\mathbf{v})]$ . All problems in the fluid limit, present in models in which the separation of fluid and solid particle trajectories was considered without accounting for the geometry of the process [16] are clearly avoided: when inertia and gravity are sent to zero, the fluid case described by Eqns. (55-56) is automatically recovered.

We can easily estimate the turbophoretic drift, i.e. the component of particle transport due to the turbulence intensity gradient [29, 30]. Multiplying Eqn. (60) by  $v^i$  and integrating in  $\mathbf{v}$  and  $\mathbf{u}$  we obtain at stationary state and for uniform concentration  $\partial_j \langle v^i v^j \rangle = \langle F^i(\mathbf{v}, \mathbf{u}) \rangle$ , which, for linear  $F^i$ , can be inverted to obtain  $\langle v^i \rangle$ . In the Stokesian case described by Eqn. (60), and small Stokes number  $St = \tau_S/\tau_E$ , we can approximate  $\langle v^i v^j \rangle = R^{ij}$ , and we obtain:

$$\langle v^i \rangle = -\tau_S \partial_j R^{ij} \quad (61)$$

## VII. Lagrangian one-time statistics and ergodic properties

As discussed at the end of Section II, we can imagine Eqn. (8) as giving the local behaviour of a random velocity field whose restriction to straight lines in space-time are Markovian processes. This allowed to have a random velocity field with Eulerian correlations in time and space, which are both well defined and easy to calculate. Unfortunately, unless the  $a \rightarrow 0$  limit of the Kraichnan model is considered [25], it is not possible to hypothesize at the same time a Markovian behaviour along trajectories. In consequence of this, the Lagrangian statistics becomes a complicated business.

However, it turns out that different statistical quantities are affected by the presence of memory in qualitative different ways and there are situations in which

Markovianization of the trajectories becomes appropriate. Let us try to understand what happens in detail.

The central quantity one needs for a description of Lagrangian statistics are conditional probabilities in the form

$$\rho(\mathbf{X}_0|\mathbf{X}_1\dots\mathbf{X}_n) \quad (62)$$

where  $\mathbf{X}_k \equiv \mathbf{X}(t_k) \equiv \{\mathbf{u}(\mathbf{x}(t_k), t_k), \mathbf{x}(t_k)\}$ ,  $k = 0, \dots, n$ . Let us consider for now the simplest case of a passive tracer. Such conditional probabilities could be obtained ideally by carrying on a Montecarlo of trajectories originating from  $\{t_n, \mathbf{X}_n\}$  and sampling the particle positions and velocities at  $t = t_k$ ,  $k = n - 1, \dots, 1$ . Let us focus on the case  $n = 1$ , which presents already all the difficulties due to memory. Actually, the transition probability  $\rho(\mathbf{X}_0|\mathbf{X}_1)$  gives precisely the evolution of a cloud of tracers from an instantaneous release, i.e. a puff; from the same transition probability, also the Lagrangian correlation time could be determined and the calculation will be illustrated in the next section. Suppose we have a set of trajectories starting at time  $t_1$  with initial condition  $\mathbf{X}_1$ , whose form is known up to time  $t$ . This allows us to reconstruct  $\rho_L(\mathbf{X}(t)|\mathbf{X}_1)$ . The conditional probability at the instant  $t + dt$  will be given by the formula:

$$\begin{aligned} & \rho_L(\mathbf{X}(t + dt)|\mathbf{X}_1) \\ &= \int d^6 X(t) \rho_L(\mathbf{X}(t + dt)|\mathbf{X}(t), \mathbf{X}_1) \rho_L(\mathbf{X}(t)|\mathbf{X}_1) \end{aligned} \quad (63)$$

which corresponds to first summing all the trajectories going from  $\{t_1, \mathbf{X}_1\}$  to  $\{t + dt, \mathbf{X}(t + dt)\}$  passing through  $\{t, \mathbf{X}(t)\}$ , and then summing over  $\mathbf{X}(t)$ . Now, to determine  $\rho(\mathbf{X}(t + dt)|\mathbf{X}(t), \mathbf{X}_1)$ , we could average first on the part of the trajectories going from  $\{t_1, \mathbf{X}_1\}$  to  $\{t, \mathbf{X}(t)\}$  and then on that going from  $\{t, \mathbf{X}(t)\}$  to  $\{t + dt, \mathbf{X}(t + dt)\}$ . From the point of view of a Montecarlo, this means that we can consider an ensemble of fictitious trajectories whose dynamics is only conditioned to the initial condition  $\{t_1, \mathbf{X}_1\}$  and to the current position  $\{t, \mathbf{X}(t)\}$ .

We thus reach the not so obvious conclusion that, to determine the evolution of a PDF with conditions at  $n$  previous instants, we need to study a dynamics conditioned to  $n + 1$  instants, but we do not need the whole trajectory history. Because

of this, if we are interested in a 1-time PDF, Markovianization of the dynamics will be an appropriate procedure.

This fact allows us to verify analytically that the 1-point velocity PDF sampled by a passive tracer coincides with the Eulerian PDF; in other words the ergodic property one expects from incompressibility is satisfied.

In the case of a passive tracer,  $dx^\mu = \{dt, \mathbf{u}dt\}$  where  $\mathbf{u}(t)$  identifies the fluid velocity sampled by the moving particle, and Eqns. (55) and (56) will be the Langevin and Fokker-Planck equations associated with the Markovianized dynamics. From incompressibility [see Eqn. (12)], and from the properties of the drift components  $\bar{A}$ ,  $\Phi$  and  $\Psi$  [see Eqns. (18-21)], we can write:

$$(\partial_t + \mathbf{u} \cdot \nabla)\rho_L + \partial_{u^i}\Phi_0^i + u^j\partial_{u^i}\Phi_j^i = -\partial_{u^i}[(\bar{A}_j^i u^j + \bar{A}_0^i - \frac{1}{2}\mathcal{B}^{ik}\partial_{u^k})\rho_L] \quad (64)$$

Setting  $\rho_L = \rho_E$ , from Eqns. (19) and the time component of Eqn. (20), Eqn. (64) reduces to  $u^i\partial_i\rho_E = -u^j\partial_{u^i}\Phi_j^i$ , which, from Eqn. (20), is an identity. The ergodic property is thus satisfied.

We can repeat the calculation to check for departures from ergodicity in the solid particle case. Ergodicity means in this case that the fluid velocity distribution sampled by the solid particle

$$\bar{\rho}_L(\mathbf{u}|\mathbf{x}) = \int \rho_L(\mathbf{u}, \mathbf{v}|\mathbf{x})d\mathbf{v} \quad (65)$$

coincides with  $\rho_E(\mathbf{u}, \mathbf{x})$ . In all the Montecarlo simulations that we have carried on, described in detail in Section IX, we have found that, contrary to our expectations, ergodicity was satisfied by solid particles in isotropic homogeneous conditions. The mechanism seems to be the following.

In homogeneous stationary conditions, the Fokker-Planck equation for the distribution  $\rho_L(\mathbf{u}, \mathbf{v})$  will read, from Eqn. (60):

$$\partial_{v^i}(F^i\rho_L) + \partial_{u^i}[(\mathbf{v} \cdot \mathbf{A}^i + A_0^i)\rho_L] = \frac{1}{2}\partial_{u^i}\partial_{u^j}\mathcal{B}^{ij}\rho_L \quad (66)$$

where  $\mathcal{B}^{ij} = \mathcal{B}^{ij}(\mathbf{v})$ . Exploiting well-mixedness [see Eqn. (19)] and setting from isotropy  $\Xi = 0$ , this equation can be rewritten in the form:

$$\partial_{v^i}(F^i\rho_L) + \partial_{u^i}[\frac{1}{2}\mathcal{B}^{ij}(\partial_{u^j}\rho_L - \rho_L\partial_{u^j}\log\rho_E)] = 0 \quad (67)$$

and, integrating in  $d^3v$ , we reach the following equation for the deviation from ergodicity:

$$\partial_{u^i}[\bar{\rho}_L(\langle \mathcal{B}^{ij} | \mathbf{u} \rangle \partial_{u^j} \log \bar{\rho}_L / \rho_E + \partial_{u^j} \langle \mathcal{B}^{ij} | \mathbf{u} \rangle)] = 0 \quad (68)$$

We see that non-ergodic behaviours are associated with the divergence of the average over solid particle trajectories of the velocity structure function:

$$\partial_{u^j} \langle \mathcal{B}^{ij} | \mathbf{u} \rangle = \int d^3v \partial_{u^j} \rho_L(\mathbf{v} | \mathbf{u}) \mathcal{B}^{ij}(\mathbf{v}) \quad (69)$$

In the case of solid particles, for which  $\langle \mathcal{B}^{ij} | \mathbf{u} \rangle \neq \mathcal{B}^{ij}(\mathbf{u})$ , we would expect in general  $\partial_{u^j} \langle \mathcal{B}^{ij} | \mathbf{u} \rangle \neq 0$ . This turns out not to be true, however, when turbulence is isotropic. Let us show how this happens.

We can decompose  $\nabla_u \rho_L(\mathbf{v} | \mathbf{u})$  in spherical vectors depending on  $\mathbf{v}$  [see Eqns. (B7-B8)]:

$$\nabla_u \rho_L(\mathbf{v} | \mathbf{u}) = \rho_{01} \mathbf{v} + \rho_{11}(\mathbf{u} \cdot \mathbf{v}) \mathbf{v} + \rho_{12} \mathbf{u} + \dots \quad (70)$$

where, from isotropy,  $\rho_{lk} = \rho_{lk}(|\mathbf{v}|, |\mathbf{u}|)$ . Higher harmonics (not indicated) are by construction orthogonal (see Appendix B). From Eqn. (38), we see that only the term

$$\mathbf{h} = \rho_{11}(\mathbf{u} \cdot \mathbf{v}) \mathbf{u} + \rho_{12} \mathbf{u} \quad (71)$$

can contribute to  $\partial_{u^j} \langle \mathcal{B}^{ij} | \mathbf{u} \rangle$ . In order for this contribution to be zero, it is sufficient that the curl with respect to  $\mathbf{v}$  of  $\mathbf{h}$  be identically zero:

$$[|\mathbf{v}|^{-1} \partial_{|\mathbf{v}|} \rho_{12} - \rho_{11}] \mathbf{v} \times \mathbf{u} = 0 \quad (72)$$

so that  $\mathbf{h}$  can be written in the form of a potential term  $\nabla_v g(\mathbf{u}, \mathbf{v})$ , and, substituting into Eqn. (69) and integrating by parts:

$$\partial_{u^j} \langle \mathcal{B}^{ij} | \mathbf{u} \rangle = - \int d^3v g(\mathbf{u}, \mathbf{v}) \partial_{v^j} \mathcal{B}^{ij}(\mathbf{v}) = 0.$$

Now, we can obtain Eqn. (72) simply by imposing the condition, from isotropy:

$$\partial_{u^i} \langle |\mathbf{v}|^n v^j v^k | \mathbf{u} \rangle = \partial_{u^j} \langle |\mathbf{v}|^n v^i v^k | \mathbf{u} \rangle, \quad (73)$$

with  $i \neq j \neq k$  and  $n \geq 0$ . In fact, writing the averages in explicit form, Eqn. (73) can be shown to be equivalent to:

$$\int d^3v |\mathbf{v}|^{n+1} v^k [\partial_{v^i} \partial_{u^j} - \partial_{v^j} \partial_{u^i}] \rho_L(\mathbf{v} | \mathbf{u}) \quad (74)$$

and again, from orthogonality of the decomposition, only the  $\rho_{11}$  and  $\rho_{12}$  terms in  $\nabla_u \rho_L$  could contribute. Hence, exploiting the fact that  $\rho_{ij}$  depends only on  $|\mathbf{u}|$  and  $|\mathbf{v}|$ , Eqn. (74) becomes equivalent to

$$\int d^3v [|\mathbf{v}|^{-1} \partial_{|\mathbf{v}|} \rho_{12} - \rho_{11}] |\mathbf{v}|^{n+1} = 0$$

which implies Eqn. (72) and satisfaction of the ergodic property.

## VIII. Two-time statistics and the Lagrangian correlation time

Explicit determination of the Lagrangian dynamics taking into account memory of an initial condition is possible when the  $\mathbf{u}(\mathbf{x}, t)$  is isotropic, homogeneous and Gaussian. It thus becomes possible to estimate the error implied in the Markovianization of the trajectories. The simplest estimator is the Lagrangian correlation time

$$\tau_L = \frac{1}{3u_T^2} \int_0^\infty dt \langle \mathbf{u}(t) \cdot \mathbf{u}(0) \rangle \quad (75)$$

where  $\mathbf{u}(t) \equiv \mathbf{u}(\mathbf{x}(t), t)$  and we are considering passive tracers. As discussed at the start of the previous section, we need an evolution equation for the trajectory  $\{\mathbf{u}(t), \mathbf{x}(t)\}$ , given an initial condition at  $t = 0$  [for simplicity, fix  $\mathbf{x}(0) = 0$ ]. The starting point is the following decomposition for the tracer velocity:

$$\mathbf{u}(t + \Delta) = \langle \mathbf{u}(t + \Delta) | \mathbf{u}(t), \mathbf{x}(t); \mathbf{u}(0), 0 \rangle + \Delta \mathbf{w} \quad (76)$$

plus knowledge of the conditional averages:

$$\langle \mathbf{u}(t + \Delta) | \mathbf{u}(t), \mathbf{x}(t); \mathbf{u}(0), 0 \rangle \quad \text{and} \quad \langle \Delta \mathbf{w} \Delta \mathbf{w} | \mathbf{u}(t), \mathbf{x}(t); \mathbf{u}(0), 0 \rangle \quad (77)$$

As discussed in detail in Appendix C, these averages can be obtained from the correlation between velocities at  $\{0, 0\}$ ,  $\{t, \mathbf{x}(t)\}$  and  $\{t + \Delta, \mathbf{x}(t + \Delta)\}$ . We identify correlations between points on a trajectory by:

$$\hat{C}^{ij}(\Delta) = \langle u^i(t) u^j(t + \Delta) \rangle, \quad (78)$$

If  $\mathbf{u}$  is Gaussian, homogeneous and isotropic, these correlations can be expressed in analytical form. The mean rate of fluid velocity change along a generic space-time

direction  $\{1, \mathbf{V}\}$  will in this case take the form:

$$A_0^i + V^j A_j^i = -\frac{1}{\tau_E} \left[ \left(1 + a \frac{|\mathbf{V}|}{u_T}\right) u_\perp^i + \left(1 + a \frac{2|\mathbf{V}|}{3u_T}\right) u_\parallel^i \right] \quad (79)$$

where  $\mathbf{u}_\perp$  and  $\mathbf{u}_\parallel$  are the components of  $\mathbf{u}$  perpendicular and parallel to the fixed direction  $\mathbf{V}$ , and we have used Eqns. (29), (30) and (38), and the expression  $R^{ij} = u_T^2 \delta^{ij}$ .

Solving the equations for the correlation function along  $\{1, \mathbf{V}\}$ :

$$\frac{d}{dt} \langle u^i(\mathbf{V}t, t) u^j(0, 0) \rangle = \langle [A_0^i + V^j A_j^i] u^j(0, 0) \rangle \quad (80)$$

and introducing longitudinal and transverse projectors

$$\Pi_\parallel^{ij}(\mathbf{V}) = \frac{V^i V^j}{|\mathbf{V}|^2}, \quad \Pi_\perp^{ij}(\mathbf{V}) = \delta^{ij} - \Pi_\parallel^{ij}(\mathbf{V}) \quad (81)$$

we obtain:

$$\langle u^i(\mathbf{V}t, t) u^j(0, 0) \rangle = \Pi_\perp^{ij}(\mathbf{V}) C_{V\perp}(t) + \Pi_\parallel^{ij}(\mathbf{V}) C_{V\parallel}(t) \quad (82)$$

where

$$C_{V\perp}(t) = u_T^2 \exp\left(-\left(1 + \frac{a|\mathbf{V}|}{u_T}\right) \frac{t}{\tau_E}\right) \quad (83)$$

and

$$C_{V\parallel}(t) = u_T^2 \exp\left(-\left(1 + a \frac{2|\mathbf{V}|}{3u_T}\right) \frac{t}{\tau_E}\right) \quad (84)$$

We shall need also the inverse  $D_{ij}(t_l - t_m)$  of the correlation matrix  $\langle u^i(t_l) u^j(t_m) \rangle$ ,  $l, m = 1, 2$ ;  $t_1 = 0$ ,  $t_2 = t$ , defined by the relation:

$$\sum_m D_{ij}(t_l - t_m) \langle u^j(t_m) u^k(t_n) \rangle = \sum_m \langle u^k(t_n) u^j(t_m) \rangle D_{ji}(t_m - t_l) = \delta_i^k \delta_{ln} \quad (85)$$

From Eqns. (82-84), we find:

$$D_{ij}(t_l - t_m) = \Pi_{ij}^\perp(\mathbf{U}) D_\perp(t_l - t_m) + \Pi_{ij}^\parallel(\mathbf{U}) D_\parallel(t_l - t_m) \quad (86)$$

where  $\mathbf{U} = \mathbf{u}(t) - \mathbf{u}(0)$ ,

$$D_\perp = \frac{1}{C_{U\perp}^2(0) - C_{U\perp}^2(t)} \begin{pmatrix} C_{U\perp}(0) & -C_{U\perp}(t) \\ -C_{U\perp}(t) & C_{U\perp}(0) \end{pmatrix} \quad (87)$$

and we have similar expression for  $D_{\parallel}$ . At this point, we can obtain from Eqn. (C7) the expression for the average evolution of the velocity along a trajectory, conditioned to an initial condition at time zero:

$$\begin{aligned} \langle u^i(t + \Delta) | \mathbf{u}(t), \mathbf{x}(t); \mathbf{u}(0), 0 \rangle &= [\hat{C}^{ij}(\Delta) D_{jk}(t) + \hat{C}^{ij}(t + \Delta) D_{jk}(0)] u^k(0) \\ &+ [C^{ij}(\Delta) D_{jk}(0) + C^{ij}(t + \Delta) D_{jk}(t)] u^k(t) \end{aligned} \quad (88)$$

As obvious, memory of the initial condition at time zero is lost when  $t \rightarrow \infty$ . Notice that, if all points  $\{0, 0\}$ ,  $\{t, \mathbf{x}(t)\}$  and  $\{t + \Delta, \mathbf{x}(t + \Delta)\}$  are aligned along the same space-time direction  $\{1, \mathbf{V}\}$ , all the  $\Pi_{\parallel}$  and  $\Pi_{\perp}$  entering the correlation functions in Eqn. (86) will project along or perpendicular the same vector  $\mathbf{V}$ . In this case the components of  $\mathbf{u}$  parallel and perpendicular to  $\mathbf{V}$  decouple and the indices disappear; for instance:

$$\begin{aligned} \langle u_{\parallel}(t + \Delta) | \mathbf{u}(t), \mathbf{x}(t); \mathbf{u}(0), 0 \rangle &= [C_{V\parallel}(\Delta) D_{V\parallel}(t) + C_{V\parallel}(t + \Delta) D_{V\parallel}(0)] u_{\parallel}(0) \\ &+ [C_{V\parallel}(\Delta) D_{V\parallel}(0) + C_{V\parallel}(t + \Delta) D_{V\parallel}(t)] u_{\parallel}(t) \end{aligned} \quad (89)$$

and all the correlations have the same decay rate fixed by Eqn. (84). It is then easy to show that the first term on the RHS of Eqn. (89) disappears and we have

$$\langle u_{\parallel}(t + \Delta) | \mathbf{u}(t), \mathbf{x}(t); \mathbf{u}(0), 0 \rangle = u_{\parallel}(t) \exp \left( - \left( 1 + a \frac{2|\mathbf{V}|}{3u_T} \right) \frac{\Delta}{\tau_E} \right) \quad (90)$$

Hence  $\langle u_{\parallel}(t + \Delta) | \mathbf{u}(t), \mathbf{x}(t); \mathbf{u}(0), 0 \rangle = \langle u_{\parallel}(t + \Delta) | \mathbf{u}(t), \mathbf{x}(t) \rangle$ . If the trajectory is developing along a straight line, we will recover Markovian statistics as required.

Expressing  $\Delta \mathbf{w}$  as the difference between  $\langle \mathbf{u}(t + \Delta) | \mathbf{u}(t), \mathbf{x}(t); \mathbf{u}(0), 0 \rangle$  and  $\mathbf{u}(t + \Delta)$ , and substituting into Eqn. (C8), we obtain instead, for the fluctuation term:

$$\langle \Delta w^i \Delta w^j | \mathbf{u}(t), \mathbf{x}(t); \mathbf{u}(0), 0 \rangle = C^{ij}(0) - D_{kl}(0) C^{li}(\Delta) C^{kj}(\Delta) \quad (91)$$

In Figure 2 we compare the result of a Montecarlo for the Lagrangian correlation time Eqn. (75) using the exact dynamics described by Eqns. (76), (88) and (91), with that obtained from the Markovianized version given by Eqn. (55). As could

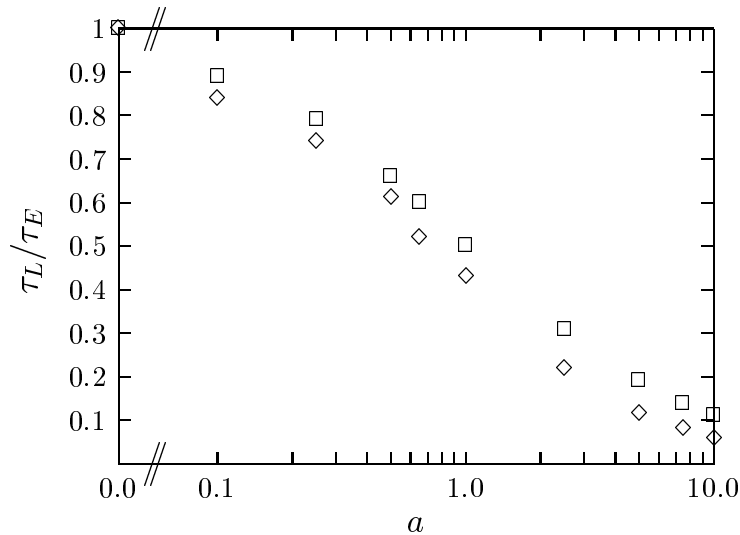


Figure 2: Dependence of the Lagrangian correlation time on the ratio  $a$  between eddy life time and eddy rotation time;  $\square$  exact;  $\diamond$  Markovian approximation.

be guessed, the Markovian approximation becomes exact in the  $a = 0$  limit, when the trajectory, in a correlation time, remains close to the time line  $\{1, 0\}$ . At least in this case, the choice given by Eqn. (15), of Markovian statistics along rectilinear cuts in space-time, is the most appropriate.

## IX. Solid particle transport in homogeneous isotropic turbulence

Inertia and crossing trajectory effects determine a substantial change in the statistics of fluid velocities sampled by the solid particle with respect to that of passive tracer velocities.

Several authors reserved particular attention to the long time behaviour of correlation functions of sampled fluid velocities and long-time particle diffusion coefficients [10, 11, 31, 32].

Following Csanady [10], Sawford and Guest [12] kept into account the effect of gravity produced trajectory crossing by a suitable assumption on the renormalization of the correlation time of the fluid velocity sampled by the falling particle. Their

model was applied to grid-generated turbulence and their results were found to agree with experimental wind tunnel data. It is not clear, however, how much this approach can be extended to generic non-homogeneous and non-stationary turbulent flows, especially in the case of strong turbulence gradients [33].

Free-flight models [13] (see also [34] for a brief review) are known to make unphysical assumptions about the velocity that particles assume when they are projected towards the wall from the buffer and logarithmic regions. As regards the eddy-interaction model of Kallio and Reeks [34], this has been shown in [35] not to satisfy the well-mixedness condition. The model described in [35] improved this aspect, but without reproducing the build-up of concentration. The issue, to be discussed in the next section, is the difficulty in isolating near wall solid particle accumulation effects from spurious concentration build-up from improper treatment of the well-mixedness condition.

A recent advance was obtained in [36], but in this approach a turbophoretic force had to be introduced from the outside, whereas in our approach the turbophoretic flux results in self-consistent way from the dynamics [see Eqn. (61)].

The central role in the solid particle dispersion is played by the correlation time  $\tau'_L$ , of the fluid velocity sampled by the solid particles. In particular, with  $\tau'_L(\parallel)$  we indicate the longitudinal effective Lagrangian time, i.e., along the direction of gravity, and with  $\tau'_L(\perp)$  the transverse effective Lagrangian time.

Let us briefly summarize the main properties of  $\tau'_L(i)$ . When gravity is dominant ( $v_G \gg u_T$ ), the correlation function of sampled fluid velocities decays faster than that of passive tracers and  $\tau'_L(i) < \tau_L$ , where  $i$  is referred to longitudinal ( $\parallel$ ) or transverse ( $\perp$ ) [10, 11]. Taking  $v_G = g\tau_S$  with  $g$  fixed, we see that  $\tau'_L(i)$  decreases from the value  $\tau_L$ , corresponding to  $\tau_S = 0$ , to zero as  $\tau_S$  increases. Furthermore, the correlation functions do not decay in the same way in all directions. Due to the continuity effect described in [10], the decay is slower in the direction of gravity, so that the longitudinal Lagrangian time  $\tau'_L(\parallel)$  is longer than the transverse one  $\tau'_L(\perp)$ .

In the inertia dominated case ( $v_G \ll u_T$ ), the sampled correlation function decays slower than that of passive tracer velocities and  $\tau'_L > \tau_L$ . The limit  $\tau_S \rightarrow 0$  is the same as above, but now  $\tau'_L$  increases with  $\tau_S$  and, in the limit  $\tau_S \rightarrow \infty$ , tends to the

Eulerian time scale  $\tau_E$  [11, 31].

We will show shortly how all these effects are automatically reproduced in our approach.

We consider a Gaussian homogeneous isotropic zero-mean random velocity field. Thus, the drift term  $\bar{A}_\mu^i$  is given by Eqn. (30) with  $S^{ij} = \delta^{ij}/u_T^2$ , the PDF is given by Eqn. (29) and the noise tensor is isotropic [see Eqn. (38)]. The terms  $\Phi_\mu^i$  and  $\Psi_j^i$  are zero for homogeneity and the gauge terms  $\Xi_\mu^i$  are zero for isotropy.

From now on in this section, we rewrite the equations expressing the velocities  $\mathbf{u}$  and  $\mathbf{v}$  and time  $t$  in units of  $u_T$  and  $\tau_E$  respectively. Note that, in this way,  $\tau_S$  becomes equivalent to the Stokes number  $St$  [27], i.e., the ratio between the Stokes time and a flow time scale ( $\tau_E$  in this case). As regards gravity, it results  $v_G = St/Fr$ , being  $Fr = g \tau_E/u_T$  the Froude number related to the magnitude of the gravity  $g$  with respect to turbulence scales [11]. We consider Eqns. (8), (30) and (38) with  $dx^\mu = (dt, \mathbf{v}dt)$ , being  $\mathbf{v}$  the particle velocity whose dynamics is given by Eqn.(58). Then, we have a set of model equations for the solid particle transport:

$$\begin{cases} du^i = -(1 + a |\mathbf{v}|)u^i dt + \frac{a}{6}v^j u_j \hat{v}^i dt + dw^i \\ \langle dw^i dw^j \rangle = 2 [(1 + a |\mathbf{v}|) \delta^{ij} - \frac{a}{3}|\mathbf{v}| \hat{v}^i \hat{v}^j] dt \end{cases} \quad (92)$$

being  $\hat{\mathbf{v}} = \mathbf{v}/|\mathbf{v}|$ . Applying to Eqn. (92) the projectors defined in Eqn. (81), with  $\mathbf{V} = \mathbf{v}$ , it is easily seen that  $d\mathbf{u}$  is split into a longitudinal and a transverse component, characterized by different values of the drift:  $1 + 2/3 a|\mathbf{v}|$  for the fluid velocity component parallel to the particle velocity and  $1 + a|\mathbf{v}|$  for the normal component. As the role of gravity increases, the symmetry breaking of particle motion due to the presence of a preferential direction, i.e., the direction of gravity, involves a separation between the longitudinal and transverse time scale (continuity effect). In the gravity dominated case,  $v_G \gg 1$ , we have  $|\mathbf{v}| \simeq v_G$ , with the result:

$$\tau'_L(\parallel) \simeq \frac{3}{2av_G}; \quad \tau'_L(\perp) \simeq \frac{1}{av_G}; \quad \frac{\tau'_L(\parallel)}{\tau'_L(\perp)} = \frac{3}{2} \quad (93)$$

It is difficult to obtain an analytical solution for the PDF  $\rho_L(\mathbf{u}, \mathbf{v})$  and the velocity correlation functions  $\langle u^i(t)u^j(0) \rangle$  because of the multiplicative noise. For this reason, numerical simulations by means of Montecarlo technique have been performed to

obtain solutions of Eqns. (58) and (92). Following Yeung and Pope [37] (see also [38]), we choose a value  $\tau_L/\tau_E \approx 0.5$ , which, from Figure 2, corresponds to  $a = 0.65$ .

As mentioned in Section VII, the ergodic property has been verified to hold also in the solid particle case. Both in the case of Gaussian statistics and of an isotropic kurtosis described by Eqn. (A3) (see Appendix A), with and without gravity, the marginal Lagrangian PDF  $\bar{\rho}_L(\mathbf{u})$  defined in Eqn. (65) has been found to coincide, to within numerical error, with the Eulerian PDF  $\rho_E(\mathbf{u})$ .

In the presence of gravity, this means that the average of the sampled fluid velocity  $\langle \mathbf{u} \rangle_L$  coincides with its Eulerian counterpart  $\langle \mathbf{u} \rangle$ , which is zero, and that, therefore, no renormalization is produced on the value of the terminal velocity  $\mathbf{v}_G$ .

Another non trivial result from the numerical simulation is that the correlation functions of both passive tracers velocities ( $\tau_S = 0$  and  $v_G = 0$ ) and of sampled fluid velocities appears to decay exponentially as in the Gaussian case for standard Lagrangian models.

In Figure 3 the effective transverse Lagrangian times  $\tau'_L(\perp)$  have been plotted

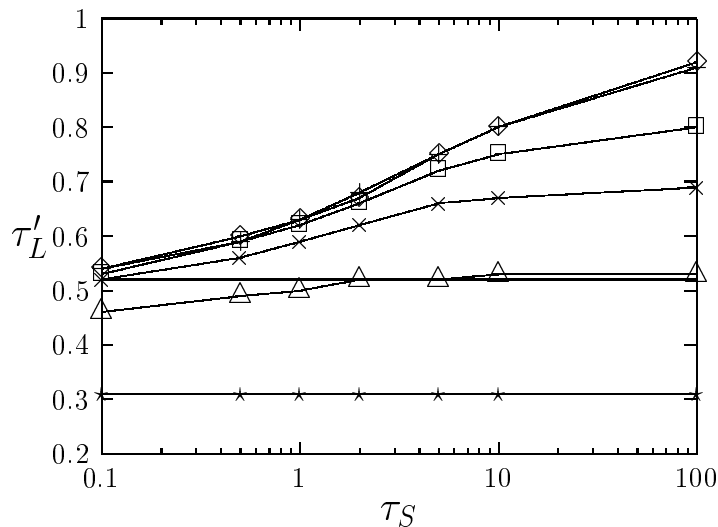


Figure 3: Behaviour of  $\tau'_L(\perp)$  as a function of the Stokes time  $\tau_S$  for different values of the adimensional terminal velocity  $v_G$  (dimensionless units).  $\diamond$   $v_G = 0$ ;  $+$   $v_G = 0.1$ ;  $\square$   $v_G = 0.5$ ;  $\times$   $v_G = 1$ ;  $\triangle$   $v_G = 2$ ;  $\star$   $v_G = 5$ . Reference line at  $\tau'_L = \tau_L = 0.52$ .

as function of  $\tau_S$  ( in units of  $\tau_E$ ) for different values of  $v_G$  (the Lagrangian time scale of passive tracer has been reported for a comparison). In the range  $v_G < 1$

(inertia dominant) the curves are increasing from  $\tau_L/\tau_E = 0.52$  and tend to about 1 as  $\tau_S \rightarrow \infty$  (i.e., the Lagrangian time tends to the Eulerian time). For  $v_G > 1$  (gravity dominant) the curves loose their dependence on  $\tau_S$  and the correlation time is approximately equal to the eddy crossing time given (always in dimensionless units) by  $v_G^{-1}$ . This is in agreement with the asymptotic formulae in Eqns. (93). Figure 4 shows the behaviour of  $\tau'_L(\parallel)$  and  $\tau'_L(\perp)$  as function of  $v_G$  for fixed  $\tau_S$ . As

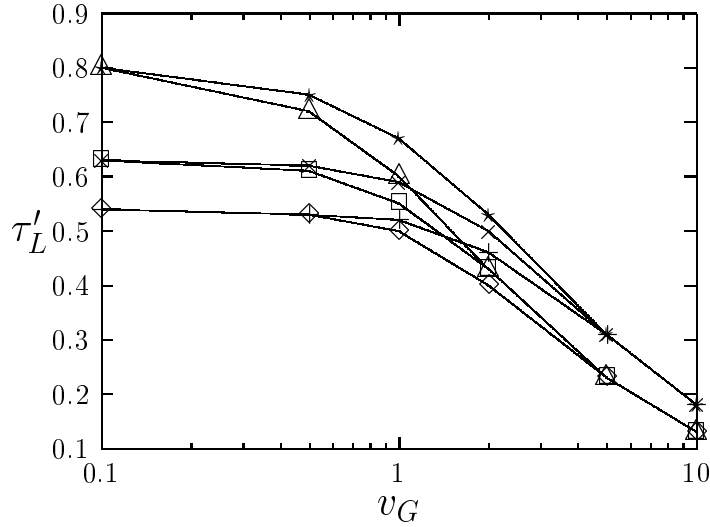


Figure 4: Behaviour of  $\tau'_L(\parallel)$  and  $\tau'_L(\perp)$  as a function of the terminal velocity  $v_G$  = for different values of  $\tau_S$  (dimensionless units). Longitudinal:  $\star$   $\tau_S = 10$ ;  $\times$   $\tau_S = 1$ ;  $+$   $\tau_S = 0.1$ . Transverse:  $\triangle$   $\tau_S = 10$ ;  $\square$   $\tau_S = 1$ ;  $\diamond$   $\tau_S = 0.1$ .

expected, each curve tends to a constant value in the limit  $v_G \rightarrow 0$ . The longitudinal times are always longer than the transverse ones and, in the limit  $v_G \rightarrow \infty$ , they collapse onto two different curves, whose ratio is 3/2 as predicted by Eqn. (93).

An exponential decay of the sampled fluid velocity correlation function allows easy analytical calculation of the correlation function for  $\mathbf{v}$  [31, 32, 39]. The last one reads, for  $i = \parallel, \perp$ :

$$C_p^i(t) = \langle v^i(t)v^i(0) \rangle = C_p^i(0) \left[ e^{-t/\tau_S} + \frac{e^{-t/\tau'_L(i)} - e^{-t/\tau_S}}{1 - \tau_S/\tau'_L(i)} \right] \quad (94)$$

The particle correlation time  $\tau_p(i)$  can then be calculated

$$\tau_p(i) = \int_0^\infty \frac{C_p^i(t)}{C_p^i(0)} dt = \tau_S + \tau'_L(i) \quad (95)$$

By using Taylor's theorem, the (long-time) diffusion coefficients

$$\kappa(i) = \frac{1}{2} \lim_{t \rightarrow \infty} \frac{1}{t} \langle (x_i(t) - x_i(0))^2 \rangle, \quad i = \parallel, \perp \quad (96)$$

can be expressed in terms of the Lagrangian correlation times for  $\mathbf{v}$  as follows

$$t \gg \tau_p(i) : \quad \kappa(i) = \tau_p(i) C_p^i(0) = \tau_L'(i) \quad (97)$$

Thus, the diffusion coefficients  $\kappa(i)$  will behave exactly as the effective Lagrangian times  $\tau_L'(i)$ . The adimensional diffusion coefficient of passive tracers is simply given by  $\kappa = \tau_L = 0.52$ . Hence, in agreement with [11],  $\kappa(i)$  will be larger than in the passive scalar case when inertia is dominant, smaller when gravity is dominant. Furthermore, when gravity is dominant, the longitudinal solid particle diffusion coefficient will be larger than the transverse one.

## X. Solid particle transport in turbulent channel flow

We focus in this section on phenomena of accumulation and deposition associated with the interaction of inertial particles with the inhomogeneity of the flow and the presence of solid boundaries. Starting from the work of McLaughlin [40], the reference situation that is typically considered, both to identify the main features of particle transport, and to test the functionality of transport models, is that of the turbulent channel flow. Three mechanisms have been identified to govern the deposition and accumulation processes [41]: turbulent diffusion, turbophoresis and free flight. Turbulent diffusion, giving rise to a particle flux opposite to concentration gradients, has the same meaning as in passive scalar transport. Turbophoresis [29, 30] is associated with compressibility of the particle phase and is the part of the particle flow due to the presence of turbulence gradients. Free flight [13] refers instead to the large velocity particles arriving, from the buffer and the logarithmic region, at the low turbulence regions close to the wall, where they carry on an almost ballistic kind of motion.

All these effects are expected to resent in different ways of the geometry and

the statistical properties of the turbulence, in particular the presence of coherent structures and intermittency [42, 43].

Consider a turbulent channel flow with streamwise direction  $x_1$ , spanwise direction  $x_3$  and cross-stream direction  $x_2$  (normal to the walls), and introduce standard wall variables identified where necessary with +, normalized with the friction velocity  $u_*$  and the reference length and time scales  $x_2^* = \nu/u_*$  and  $\tau_* = x_2^*/u_*$  where  $\nu$  is the kinematic viscosity.

As it is well known, the turbulent boundary layer in the channel flow can be divided into a logarithmic region ( $x_2^+ \gtrsim 30$ ), a buffer region ( $5 \lesssim x_2^+ \lesssim 30$ ) and a viscous sublayer ( $0 \lesssim x_2^+ \lesssim 5$ ), characterized by different behaviours of the mean field and the turbulence. The buffer region and the viscous sublayer are characterized by the presence of coherent structures (in particular, streaks and bursts) and by strong intermittency. In Figure 5, we give a plot from DNS (Direct Numerical Simulations) of the kurtosis of the velocity component normal to the wall [44]. Streaks, located in the viscous sublayer, are elongated regions of fluid, oriented in the

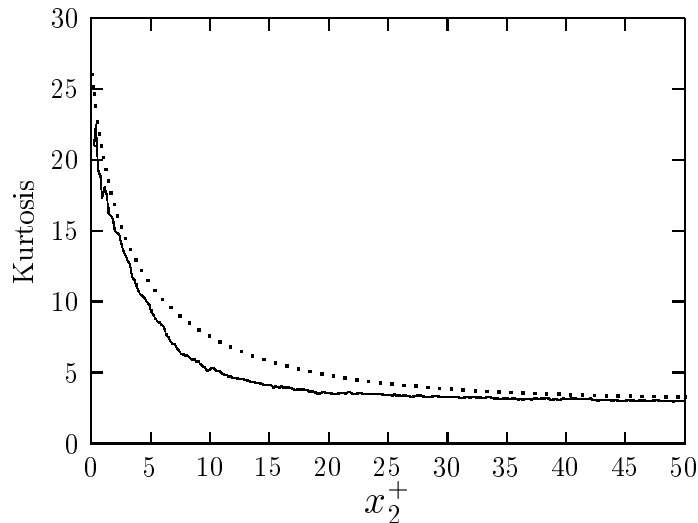


Figure 5: Comparison between DNS data for the kurtosis, taken from [44], (dotted line) and simulated data from Montecarlo (continuous line).

streamwise direction, moving slower than the mean flow; bursts are intermittent jets perpendicular to the wall, located in the buffer region, originating from instability of a streak (streak lifting, or ejection) [5, 45].

The effect of these coherent structures and of intermittency can be included in our model by means of both drift and noise terms. We shall illustrate shortly how this can be done by means of a toy model. Our goal will be, in particular, to isolate the different contributions to transport from intermittency and geometry.

As input data for our model, we utilize the 1-point statistics from the DNS by Kim, Moin and Moser [44], supported by qualitative conditions on the structure of the 2-point statistics and of the correlation function profiles. The channel width  $L_c$  is nearly 360 wall units and the Reynolds number is of order 7000.

The profile for the normal velocity kurtosis and for the Reynolds tensor from [44] are shown respectively in Figure 5 and Figure 6. We disregard the contribution

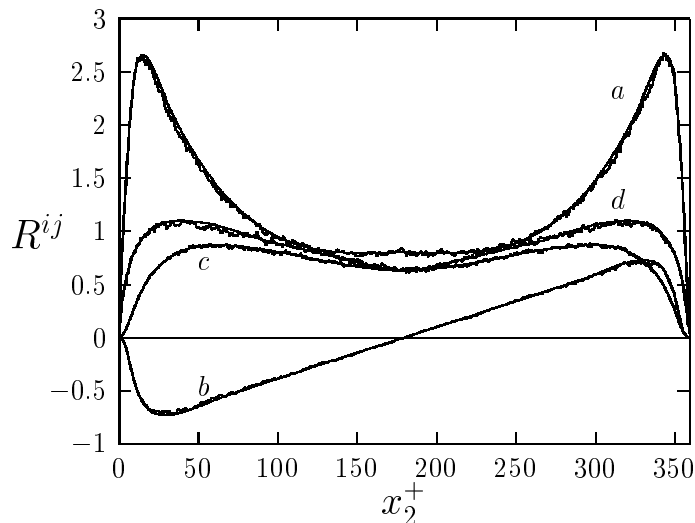


Figure 6: Comparison between input statistics for the Reynolds tensor  $R^{ij}$ , from DNS [44], and simulated data from Montecarlo. The data are almost undistinguishable: (a)  $R^{11}$ , (b)  $R^{12}$ , (c)  $R^{22}$ , (d)  $R^{33}$ .

from the velocity skewness to the statistics as well as all non-Gaussianity in the streamwise and spanwise direction, which, in any case, are smaller than the normal velocity kurtosis contribution.

For the Eulerian time scale, we set as in the previous section  $\tau_E = \frac{1}{0.52}\tau_L$  [37, 38] and use the interpolation formula:

$$\begin{cases} \tau_L = 7.122 + 0.5731 x_2^+ - 0.00129(x_2^+)^2 & x_2^+ < 140 \\ \tau_L = -19.902 + .959 x_2^+ - .00267(x_2^+)^2 & 140 < x_2^+ < 180 \end{cases} \quad (98)$$

For  $x_2^+ < 140$ , this coincides with the interpolation formula quoted in [34]. Thus, Eulerian time scales span from  $\tau_E^{max} \simeq 140$  in the channel centre to  $\tau_E^{min} \simeq 14$  at the walls.

We will not consider the effects of gravity in this section. We neglect also the effects of the Saffman lift [28] and of Brownian motion; the first one could be of some relevance in the range  $\tau_S \lesssim 10$  [34] and the second in the case of sub-micrometer particles.

We have carried on Montecarlo simulations with  $N_{tot} = 10000$  particles, uniformly distributed at the initial time. In order to obtain stationary concentration profiles after a suitable time, we introduce a source of particles at the channel centre to balance the deposition flux at the walls. As in [41], for these conditions and for quite all Stokes times, it seems that a simulation time  $T_{sim}$  of about 700 is sufficient to achieve a stationary distribution for the solid particles. Having in mind a simple estimate of the effects of coherent structures on the particle transport, we carried on simulations in four reference situations (details in Appendix D):

- i. An isotropic form of the noise term everywhere in the channel, as described by Eqn. (38), no kurtosis and no gauge term included.
- ii. Full anisotropic noise form as described by Eqns. (E1-E5), but no kurtosis and no gauge term.
- iii. Full anisotropic noise, with kurtosis taken into account, but no gauge term.
- iv. Full anisotropic noise, with kurtosis and gauge term  $\xi_0^3 \neq 0$  included.

As a validation, Figures 5-6 show that the model reproduce, in the fluid particle case, the input statistics. Furthermore, the well-mixedness condition has been shown to be satisfied (see curve f in Figure 9). This despite the possible numerical complications which could have arisen due to the presence of a multiplicative noise term. While in the case of the Reynolds tensor components input and simulated data are almost indistinguishable (see Figure 6), the agreement between the input kurtosis and the modelled one is worse, probably due to misalignment of the Reynolds tensor eigenvector with  $x_2^+$ .

We limit our analysis to some interesting values of Stokes times in the Eulerian time range:  $\tau_E^{min} \lesssim \tau_S \lesssim \tau_E^{max}$ . Being interested in the long time regime  $t \gg \max(\tau_S, \tau_E^{max})$ , we do not expect the behaviour of solid particles to change significantly in the range  $\tau_S > \tau_E^{max}$ . Conversely, in the limit  $\tau_S \ll \tau_E^{min}$ , solid particles tend to behave like fluid parcels.

We focus on the dependence of the behaviour of the concentration profile  $\theta$  and deposition flux  $J_w$ :

$$\theta = \int d^3u d^3v \rho_L(\mathbf{u}, \mathbf{v}, \mathbf{x}), \quad J_w = \frac{L_c N_d}{T_{sim} N_{tot}}$$

being  $L_c$  the channel width,  $N_d$  the number of deposited particles in the simulation time  $T_{sim}$  and  $N_{tot}$  the total number of particle simultaneously present in the channel.

As shown in Figures 7-9, a build-up of particle concentration is observed in the viscous sublayer at nearly  $x_2^+ \simeq 1$ . This, in agreement with DNS data [41, 47].

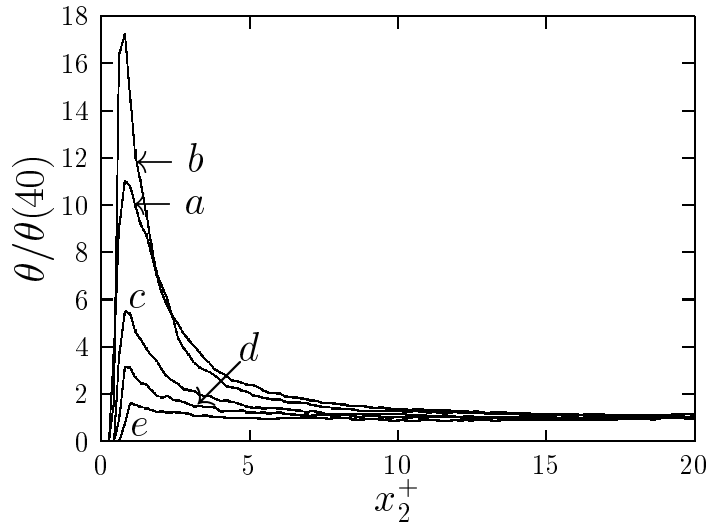


Figure 7: Concentration profile  $\theta$  vs.  $x_2^+$ . Model with isotropic noise ( $a = 0.65$ ) and Gaussian PDF.  $\Xi_\mu^i = 0$ . (a)  $\tau_S = 3$ ; (b)  $\tau_S = 10$ ; (c)  $\tau_S = 20$ ; (d)  $\tau_S = 30$ ; (e)  $\tau_S = 60$ .

The height of the concentration peaks, in the Gaussian case i, illustrated in Figure 7, agrees better with the data in [41] than with those in the open channel flow considered in [47]. In all other cases ii-iv, we obtain peak heights definitely below the results in [41].

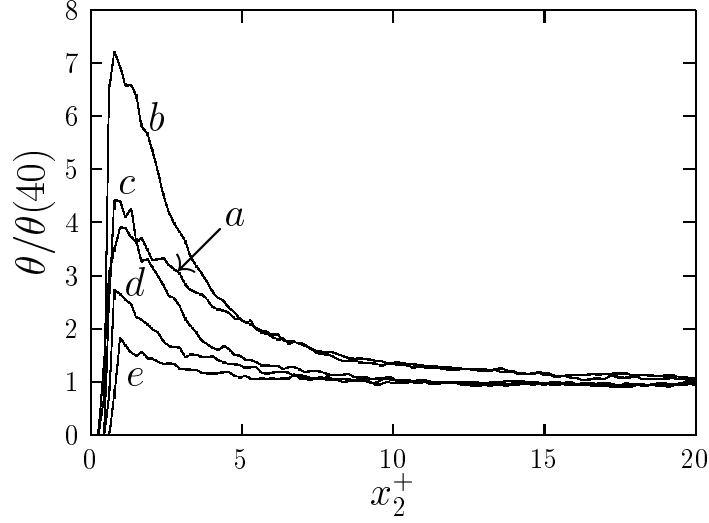


Figure 8: Concentration profile  $\theta$  vs.  $x_2^+$ . Model with anisotropic noise (coherent structures in the viscous sublayer  $\rightarrow$  bursts and streaks) and non-Gaussian PDF.  $\Xi_\mu^i = 0$ . Same values of  $\tau_S$  as in Figure 7.

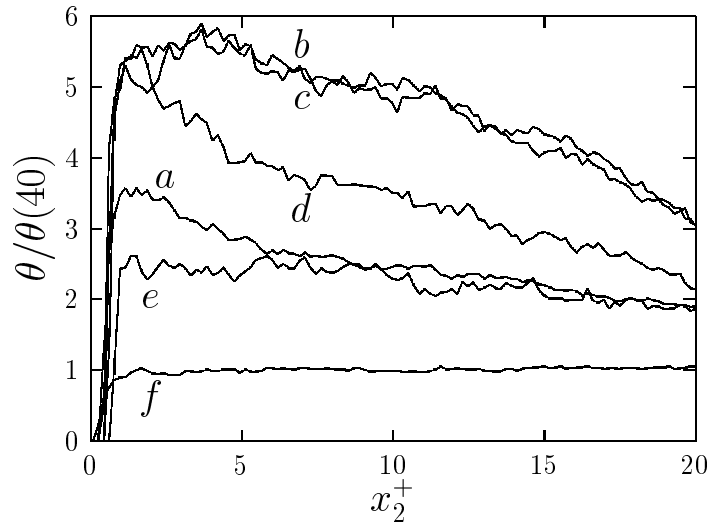


Figure 9: Concentration profile  $\theta$  vs.  $x_2^+$ . Same as figure 8, but with gauge term included. The curve denoted by (f) represents the reference concentration profile of fluid parcels.

Stokes time	isotropic Gaussian $\xi_0^3 = 0$	anisotropic Gaussian $\xi_0^3 = 0$	anisotropic bi-Gaussian $\xi_0^3 = 0$	anisotropic bi-Gaussian $\xi_0^3 = u_t^2 \max(1 - x_2^+/40, 0)$
3	11.03	2.12	3.90	3.57
10	17.23	1.97	7.20	5.89
20	5.50	1.55	4.27	5.80
30	3.14	1.31	2.74	5.29
60	1.60	1.09	1.83	2.61
120	1.28	1.09	1.09	1.55

Table I: Maximum concentration in the viscous sublayer (around  $x_2^+ \simeq 1$ ) relative to  $\theta(x_2^+ = 40)$ .

Stokes time	isotropic Gaussian $\xi_0^3 = 0$	anisotropic Gaussian $\xi_0^3 = 0$	anisotropic bi-Gaussian $\xi_0^3 = 0$	anisotropic bi-Gaussian $\xi_0^3 = u_T^2 \max(1 - x_2^+/40, 0)$
3	0.0082	0.037	0.022	0.030
10	0.10	0.13	0.083	0.048
20	0.19	0.17	0.15	0.089
30	0.22	0.20	0.19	0.15
60	0.23	0.22	0.21	0.20
120	0.23	0.22	0.22	0.22

Table II: Deposition fluxes  $J_w$ .

As regards the dependence of the height of the concentration peaks on  $\tau_S$ , we observe the presence of a maximum around  $\tau_S = 10$  (see Table I). Notice that an increase in the peak height is observed for  $\tau_S \lesssim 10$  in [41], while a decrease is observed in passing from  $\tau_S = 5$  to  $\tau_S = 15$  in [47].

Passing to the analysis of the deposition rates, we observe in all cases an increasing behaviour in function of  $\tau_S$  (see Table II). This is in qualitative agreement with observed data in the diffusion-impaction regime  $\tau_S \lesssim 15$  (see [36]), but the weak decline of deposition fluxes with increasing Stokes time [50] in the inertia-moderated regime  $\tau_S \gtrsim 15$  is not reproduced. This may be consequence of the initially uniform particle distribution that we have adopted in our simulations.

As already mentioned, in the diffusion-impaction regime, the simple Gaussian isotropic model (case i) produces a much larger build-up of concentration with respect to the other cases. As shown in Figures 10-11 this effect is decreased in the

inertia-moderated regime. It seems that, as  $\tau_S$  increases, the intermittency and geometric properties of coherent structures play a minor role. This is probably due to the fact that, as discussed in Appendix D, the transport of particles with Stokes times corresponding to Eulerian time scales above the buffer region is dominated by nearly isotropic structures.

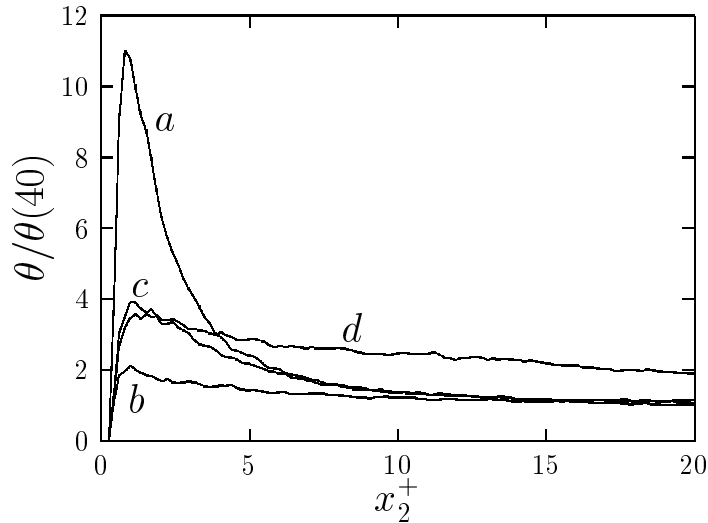


Figure 10: Concentration profile  $\theta$  vs.  $x_2^+$ . Comparison of different effects for  $\tau_S = 3$ : (a) isotropic noise and Gaussian PDF; (b) anisotropic noise and Gaussian PDF; (c) anisotropic noise and non-Gaussian PDF; (d) anisotropic noise, non-Gaussian PDF and gauge term included.

Regarding the maximum concentrations, the worse results seem to occur in case (ii). This suggests that taking into account the anisotropy of coherent structures, neglecting at the same time the associate intermittency, is not appropriate.

When inserting the gauge term (case iv), as shown in Figure 9, the general effect is that accumulation is observed not only in the viscous sublayer but also in the buffer region, possibly due the streak lifting effect being taken into account too strongly by  $\Xi$ .

## XI. Conclusions

The main result of this research is a technique which allows to derive from a random velocity field, whose correlation functions have assigned form, a class of Lagrangian

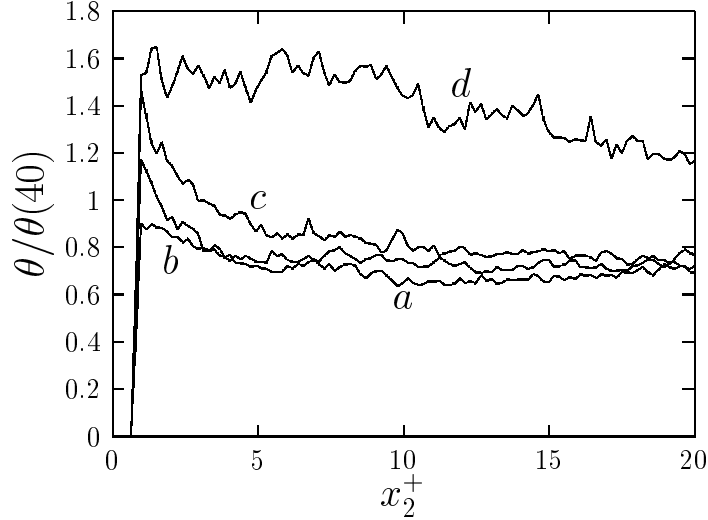


Figure 11: Same as in Figure 10 for  $\tau_S = 60$ .

models, which are identically suited to the treatment of the transport of tracer and non-tracer quantities.

This technique has the additional advantage, compared to standard Lagrangian models, that it affords consideration of the geometric structure of turbulent fluctuations, without paying any price in terms of simplicity and implementation of the well-mixedness condition. Disregarding the geometric structure of the eddies, the only free parameter remaining is the coefficient  $a$  entering Eqn. (38), whose meaning, in analogy with the inverse of  $C_0$  in standard Lagrangian models, is to give the ratio between the eddy lifetime and the eddy rotation time. At the same time, the non-uniqueness in the choice of a Lagrangian model in the standard approach, given a certain PDF  $\rho_E$ , is now turned into an advantage, allowing consideration of the antisymmetric part of the velocity correlations.

An issue that remains to be clarified is the relation between local and global random field properties: it is clear that the construction of Eqn. (15) is not unique, given the local random field properties encoded in Eqns. (8-12). Other constructions would lead to different large scale correlation structure of the random field, and to different errors in a Markovian approximation along trajectories. It remains still to be ascertained whether the choice minimizing these errors is the one provided by Eqn. (15), in which the random field is "Markovian" along rectilinear cuts in

space-time.

An alternative strategy, which would by-pass these problems, is to use the full non-Markovian approach described in Section VIII and to model the velocity correlation for the velocity at the global level. The cost in term of difficulty is not high, although the geometric interpretation in terms of noise amplitude and gauge contributions is lost. In any case, perhaps, a full non-Markovian approach is not necessary, having been possible to show that the error produced in the ratio between Lagrangian and Eulerian correlation times, in the reference situation of homogeneous isotropic turbulence and Gaussian statistics, is at most 15% in defect with respect to the exact result.

The approach that has been discussed in the present paper is based on the assumption of linear scaling in the space-time increment of the second order structure functions for the random field. Linearity was the condition for introducing generalized "four-dimensional" Langevin and Fokker-Planck equations, relating the statistics of conditional velocity increments with the one-point velocity PDF  $\rho_E$ , and for making contact with standard Lagrangian models. Justification of this approach is that accurate reproduction of the inertial range statistics is expected to be less important, for one-particle transport properties, than the large scale properties of the eddies, which are encoded in the turbulence correlation times and lengths.

Extension of the present approach beyond one-point statistics is possible in principle, but is limited by the unphysical scaling of the random field structure function at small separations. Furthermore, from Eqn. (35), all the spatial scales of the random field decorrelate with the same rate  $\tau_E$ . These characteristics can be shown to lead to a  $\Delta x \sim t^2$  scaling for the separation between pairs of fluid elements advected by the flow, in place of the correct Richardson diffusion behaviour  $\Delta x \sim t^{3/2}$ . Only concentration fluctuations on the scale of a correlation length could then be taken into account. From the formal point of view, the technique illustrated in section VIII allows, nonetheless, Montecarlo evaluation of high order correlations, without any need of Markovianization, and provides a mean of extending to finite correlation times, calculations carried on so far only in the case of the Kraichnan model [48, 49].

The fact that the transport model is determined from the statistical properties

of a random field and not of trajectories is what allowed easy extension of the model to solid particle transport.

It is to be noticed that all the properties which have been found to be satisfied by the Lagrangian correlation times for the sampled fluid velocity, in homogeneous isotropic turbulence, do not result from imposition of ad-hoc constraints on the form of the model, but simply from the kinematic properties (e.g. incompressibility) of the random field. Also in the inhomogeneous case, many important features of solid particle transport are automatically taken into account, in particular, turbophoresis.

A puzzling aspect is the fact that solid particles appear to satisfy the ergodic property in the case of a homogeneous stationary and isotropic random field. In the presence of gravity, in particular, no renormalization is produced on the settling velocity of a falling particle.

Most of these results are not expected to be sensitive to the inclusion of anisotropy in the noise and drift terms. Inclusion of these effects (coherent structures) appears instead to strongly affect particle deposition and transport in wall turbulence. We have analyzed the effect of choosing different forms of the drift and noise terms in a channel flow geometry, with the intent of getting some hints of the effect of coherent structures and intermittency on transport. The analysis in section X suggests that this is a delicate issue. For instance, taking into account anisotropy, while neglecting intermittency, has led to a model under-estimating the effect of particle accumulation, and a better functionality has been observed in the case of a simple Gaussian isotropic model, a situation already observed in [51]. An important aspect appears to be the complex interplay between non-Gaussian statistics and effective correlation times discussed in [24].

We have noticed agreement with the trends for the dependence of the deposition rates on  $\tau_S$ , observed in [41] and [52]. Within the limits of a stochastic approach like ours, we have observed rough agreement in the near wall accumulation rates, with the data of [41], but not with those of [47].

Future work will be devoted to better understanding the effect of varying the different model parameters, and to try fixing their value using DNS data.

**Acknowledgment:** We acknowledge support by Agenzia2000 grant CNR C002509\_003.

## References

- [1] G.I. Taylor "Diffusion by continuous movement", Proc. Lond. Math. Soc. **20**, 196 (1921)
- [2] A.M. Obukhov "Description of turbulence in terms of Lagrangian variables", Adv. Geophys. **6**, 113 (1959)
- [3] H. van Dop, F.T.M. Nieuwstadt and J.C.R. Hunt "Random walk models for particle displacements in inhomogeneous unsteady turbulent flows", Phys. Fluids **28**, 1639 (1985)
- [4] D.J. Thomson "Criteria for the selection of stochastic models of particle trajectories in turbulent flows", J. Fluid Mech. **180**, 529 (1987)
- [5] S.B. Pope *Turbulent flows*, (Cambridge University Press 2000)
- [6] B. Sawford "Rotation of trajectories in Lagrangian stochastic models of turbulent dispersion", Boundary Layer Meteorology **93**, 411 (1999)
- [7] A.K. Luhar and R.E. Britter "A random walk model for dispersion in inhomogeneous turbulence in a convective boundary layer", Atmospheric Environment **23**, 1911 (1989)
- [8] M.S. Borgas, T.K. Flesch and B.L. Sawford "Turbulent dispersion with broken reflectional symmetry", J. Fluid Mech. **332**, 141 (1997)
- [9] B.L. Sawford "Reynolds number effects in Lagrangian stochastic models of turbulent dispersion", Phys. Fluids A **3**, 1577 (1991)
- [10] G.T. Csanady "Turbulent diffusion of heavy particles in the atmosphere", J. Atmos. Sci. **20**, 201 (1963)
- [11] M.W. Reeks "On the dispersion of small particles suspended in an isotropic turbulent fluid", J. Fluid Mech. **83**, 529 (1977)
- [12] B.L. Sawford and F.M. Guest "Lagrangian statistical simulations of the turbulent motion of heavy particles", Boundary Layer Meteorology **54**, 147 (1991)

- [13] S.K. Friedlander and H.F. Johnstone "Deposition of suspended particles from turbulent gas streams", *Ind. Eng. Chem.* **49**, 1151 (1957)
- [14] P. Desjonqueres, A. Berlemont and G. Gousbet "A Lagrangian approach for the prediction of particle dispersion in turbulent flows", *J. Aerosol Sci.* **19**, 99 (1988)
- [15] A. Berlemont, P. Desjonqueres and G. Gousbet "Particle Lagrangian simulation in turbulent flows", *Int. J. Multiphase flow* **16**, 19 (1990)
- [16] P. Olla "Transport properties of heavy particles in high Reynolds number turbulence", *Phys. Fluids* **14**, 4266 (2002)
- [17] Y.P. Shao "A Lagrangian stochastic model for non-passive particle diffusion in turbulent flows", *Mathl. Comput. Modelling* **21**, 31 (1995)
- [18] A.M. Reynolds and J.E. Cohen "Stochastic simulation of heavy-particle trajectories in turbulent flows", *Phys. Fluids* **14**, 342 (2002)
- [19] I. Arad, V.S. L'vov and I. Procaccia "Correlation functions in isotropic and anisotropic turbulence", *Phys. Rev. E*, **59**, 6753 (1999)
- [20] C.W. Gardiner, *Handbook of Stochastic Methods* (Springer, Berlin 1985)
- [21] P.J. Holmes, J.L. Lumley, and G. Berkooz. *Turbulence, coherent structures, symmetry and dynamical systems* (Cambridge University Press, 1996)
- [22] A.C. Cohen "Estimation in mixture of two normal distributions", *Technometrics* **9**, 15 (1962)
- [23] J.H. Baerentsen and R. Berkowicz "Monte-Carlo simulation of plume dispersion in the convective boundary layer", *Atmospheric Environment* **18**, 701 (1984)
- [24] A. Maurizi, S. Lorenzani "On the influence of the Eulerian velocity PDF closure on the eddy diffusion coefficient", *Boundary Layer Meteorology* **95**, 427 (2000)
- [25] R.H. Kraichnan "Anomalous scaling of a randomly advected passive scalar", *Phys. Rev. Lett.* **72**, 1016 (1994)

- [26] L.-P. Wang and M.R. Maxey "Settling velocity and concentration distribution of heavy particles in homogeneous isotropic turbulence", *J. Fluid Mech.* **256**, 27 (1993)
- [27] M.R. Maxey and J.J. Riley "Equation of motion for a small rigid particle in a non-uniform flow", *Phys. Fluids* **26**, 883 (1983)
- [28] P.G. Saffman "The lift on a small sphere in a slow shear flow", *J. Fluid Mech.* **22**, 385 (1964)
- [29] M. Caporaloni, F. Tampieri, F. Trombetti, O. Vittori "Transfer of particles in nonisotropic air turbulence" *J. Atmos. Sci.* **32**, 565 (1975)
- [30] M.W. Reeks "The transport of discrete particles in inhomogeneous turbulence" *J. Aerosol Sci.* **14**, 729 (1983)
- [31] L.M. Pismen and A. Nir "On the motion of suspended particle in stationary homogeneous turbulence", *J. Fluid Mech.* **84**, 193 (1978)
- [32] A. Nir and L.M. Pismen "The effect of a steady drift on the dispersion of a particle in turbulent fluid" *J. Fluid Mech.* **94**, 369 (1979)
- [33] A.M. Reynolds "On the formulation of lagrangian stochastic models for heavy-particle trajectories", *J. Colloid Interface Sci.* **232**, 135 (2000)
- [34] G.A. Kallio and M.W. Reeks "A numerical simulation of particle deposition in turbulent boundary layers", *Int. J. Multiphase Flow* **15**, 433 (1989)
- [35] B.Y. Underwood "Random-walk modelling of turbulent impaction on a smooth wall", *Int. J. Multiphase Flow* **19**, 485 (1993)
- [36] A.M. Reynolds "A Lagrangian stochastic model for heavy particle deposition", *J. Colloid Interface Sci.* **215**, 85 (1999)
- [37] P.K. Yeung and S.B. Pope "Lagrangian statistics from direct numerical simulations of isotropic turbulence", *J. Fluid Mech.* **207**, 531 (1989)

- [38] Y. Sato and K. Yamamoto: "Lagrangian measurements of fluid-particle motion in an isotropic turbulent field", *J. Fluid Mech.* **175**, 183 (1987)
- [39] C.C. Meek and B.G. Jones "Studies of the behavior of heavy particles in a turbulent fluid flow", *J. Atmos. Sci.* **30**, 239 (1973)
- [40] J.B. McLaughlin "Aerosol particle deposition in numerically simulated channel flow", *Phys. Fluids A* **1**, 1211 (1989)
- [41] J.W. Brooke, T.J. Hanratty, J.B. Mc Laughlin "Free-flight mixing and deposition of aerosols", *Phys. Fluids* **6**, 3404 (1994)
- [42] J.W. Cleaver and B. Yates "Mechanism of detachment of colloidal particles from a flat substrate in a turbulent flow", *J. Colloid Interface Sci.* **44**, 464 (1973)
- [43] J.W. Cleaver and B. Yates "A sublayer model for the deposition of particles from a turbulent flow" *Chem. Eng. Sci.* **30**, 983 (1975)
- [44] J. Kim, P. Moin and R. Moser, "Turbulence in fully developed channel flow at low Reynolds number" *J. Fluid Mech.* **177**, 3990 (1987)
- [45] S.K. Robinson "Coherent motions in the turbulent boundary layer", *Annu. Rev. Fluid Mech.* **23**, 601 (1991)
- [46] L. Biferale, D. Lohse, I.M. Mazzitelli, F. Toschi "Probing structures in channel flow through SO(3) and SO(2) decomposition", *J. Fluid Mech.* **452**, 39 (2002)
- [47] C. Narayanan, D. Kakehal, L. Botto and A. Soldati "Mechanism of particle deposition in a fully developed turbulent open channel flow", *Phys. Fluids* **15**, 763 (2003)
- [48] U. Frisch, A. Mazzino and M. Vergassola, "Intermittency in passive scalar advection", *Phys. Rev. Lett.* **80**, 5532 (1998)
- [49] O. Gat, I. Procaccia and R. Zeitak "Anomalous scaling in passive scalar advection: Monte-Carlo Lagrangian trajectories", *Phys. Rev. Lett.* **80**, 5536 (1998)

- [50] M.W. Reeks and G. Skyrme "The dependence of particle deposition velocity on particle inertia in turbulent pipe flows", J. Aerosol Sci. **7**, 485 (1976)
- [51] T.K. Flesch and J.D. Wilson "A two-dimensional trajectory-simulation model for non-Gaussian, inhomogeneous turbulence within plant canopies", Boundary Layer Meteorology **61**, 349 (1992)
- [52] B.Y.H. Liu and J.K. Agarwal "Experimental observation of aerosol deposition in turbulent flow", Aerosol Sci. **5**, 145 (1974)

### Appendix A: non-Gaussian case

A symmetric one-dimensional distribution with unitary variance and kurtosis larger than three can be modelled by means of a bi-Gaussian:

$$P(x) = \frac{\alpha}{\pi^{\frac{1}{2}}} \exp(-x^2) + \frac{(1-\alpha)}{(2\pi\beta)^{\frac{1}{2}}} \exp\left(-\frac{x^2}{2\beta}\right) \quad (A1)$$

where

$$\alpha = \frac{4\langle x^4 \rangle - 12}{4\langle x^4 \rangle - 9} \quad \text{and} \quad \beta = \frac{2}{3}\langle x^4 \rangle - 1; \quad (A2)$$

parameterize the strength of the kurtosis  $\langle x^4 \rangle$ . From here, we can obtain the expression for an isotropic non-Gaussian velocity distribution:

$$\rho_E = \frac{1}{(\pi u_T^2)^{\frac{3}{2}}} \left[ \alpha \exp\left(-\frac{u^2}{u_T^2}\right) + \frac{1-\alpha}{(2\beta)^{\frac{3}{2}}} \exp\left(-\frac{u^2}{2\beta u_T^2}\right) \right] \quad (A3)$$

and for an anisotropic distribution, in which one of the velocity components, in the diagonal reference frame for the Reynolds tensor, is non-Gaussian:

$$\rho_E = \alpha \rho_1 + (1-\alpha) \rho_2 = \rho_x [\alpha \rho_{y1} + (1-\alpha) \rho_{y2}] \rho_z \quad (A4)$$

where:

$$\rho_x = \frac{1}{(2\pi \hat{R}^{11})^{\frac{1}{2}}} \exp\left(-\frac{\hat{u}_1^2}{2\hat{R}^{11}}\right), \quad \rho_z = \frac{1}{(2\pi \hat{R}^{33})^{\frac{1}{2}}} \exp\left(-\frac{\hat{u}_1^2}{2\hat{R}^{33}}\right),$$

$$\rho_{yi} = \frac{1}{(2\pi \hat{R}_i^{22})^{\frac{1}{2}}} \exp\left(-\frac{\hat{u}_2^2}{2\hat{R}_i^{22}}\right) \quad i = 1, 2 \quad (A5)$$

with  $\hat{R}_1^{22} = \hat{R}^{22}/2$ ,  $\hat{R}_2^{22} = \beta\hat{R}^{22}$ , and the hat indicating the diagonal reference frame.

Let us calculate explicitly the drift terms in the case of Eqns. (A4-A5). Substituting into Eqn. (19), we find immediately that  $\bar{A}$  is given by the superposition of the contributions from each of the Gaussians  $\rho_1$  and  $\rho_2$ :

$$\bar{A}_\mu^i dx^\mu = -\frac{1}{2\rho} \langle dw^i dw^j \rangle [\alpha \rho_1 S_{jk}^1 + (1-\alpha) \rho_2 S_{jk}^2] u^k \quad (A6)$$

(notice the absence of the hats; it is not necessary here to work in the diagonal reference frame). The contribution from the  $\Phi$  and  $\Psi$  terms has a more complicated form. Let us take the laboratory frame with the inhomogeneity direction along  $x^2$  (the usual channel flow geometry in which  $x^1$  is the mean flow direction). We use the ansatz:

$$\Phi_\mu^i = \alpha \Phi_{\mu 1}^i + (1-\alpha) \Phi_{\mu 2}^i + \Delta \Phi_\mu^i, \quad \Delta \hat{\Phi}_\mu^i = \hat{F}_\mu \delta_2^i \quad (A7)$$

where  $\Phi_1$  and  $\Phi_2$  give the form of  $\Phi$  in the case  $\rho_E = \rho_1$  and  $\rho_E = \rho_2$ . Substituting into Eqn. (20) and using Eqns. (A4-A5), we obtain:

$$\partial_{\hat{u}^2} \hat{F}_\mu = -\delta_\mu^2 \hat{\partial}_2 \alpha (\rho_1 - \rho_2) \quad (A8)$$

leading to the result in the laboratory reference frame:

$$\Delta \Phi_\mu^i = -\delta_\mu^2 \Omega^i{}_2 \frac{\rho_x \rho_y}{(2\pi)^{\frac{1}{2}}} \partial_2 \alpha \int_{\hat{u}_2/\sqrt{R_2^{22}}}^{\hat{u}_2/\sqrt{R_1^{22}}} d\hat{u} e^{-\hat{u}^2/2} \quad (A9)$$

where  $\Omega^i{}_2$  is the rotation matrix defined through  $u^i = \Omega^i{}_j \hat{u}^j$ , i.e.  $\Omega^i{}_j = \mathbf{e}^i \cdot \hat{\mathbf{e}}_j$ .

Analogous procedure is followed to obtain the  $\Psi$  term. From Eqn. (21), in analogy with Eqn. (26), write:

$$\psi^i = \alpha \psi^i + (1-\alpha) \psi^i + \Delta \psi^i \quad \Delta \hat{\psi}^i = \delta_2^i G \quad (A10)$$

where  $2\partial_{\hat{u}^i} \psi^i = -\Delta \Phi_i^i = -\hat{F}_2$ , and decompose  $\Psi_j^i$  in analogous way. From Eqn. (A9), we obtain immediately:

$$G = \frac{\rho_x \rho_y}{2(2\pi)^{\frac{1}{2}}} \Omega^2{}_2 \partial_2 \alpha \int_{-\infty}^{\hat{u}_2} d\hat{u} \int_{\hat{u}/\sqrt{R_2^{22}}}^{\hat{u}/\sqrt{R_1^{22}}} dx e^{-x^2/2} \quad (A11)$$

and, substituting again into Eqn. (26) [in real space:  $\Psi_j^i = \delta_j^i \partial_{u^k} \psi^k - \partial_{u^j} \psi^i$ ], we find:

$$\Delta \Psi_j^i = \delta_j^i \partial_{\hat{u}^2} G - \Omega^i{}_2 \Omega_j^l \partial_{\hat{u}^l} G \quad (A12)$$

Assuming that the statistics of  $d\mathbf{w}$  be independent of the velocity, as we have done in section II, has the consequence that all of the non-Gaussianity is contained in the drift. The small scale structure of the correlations, associated with  $d\mathbf{w}$  remain therefore Gaussian. This breaks, for large values of the kurtosis, the direct relationship between the drift coefficients and the correlation lengths [24]. It is easy to see what happens looking at Eqns. (A4) and (A6). Whenever the value of  $u$  goes above  $u_T$ , the slowly decaying  $\rho_2$  becomes dominant in Eqn. (A6) and leads to a reduced decay rate for the fluctuation that can thus slowly grow to produce a burst. We thus have a hierarchy of time-scales (focus for simplicity on variations along time):

$$\begin{aligned}\tau_E &\longrightarrow \text{Time scale for background } (u \sim u_T) \\ \beta\tau_E &\longrightarrow \text{Time scale for bursts } (u \sim \beta^{\frac{1}{2}}u_T) \\ \beta^2\tau_E &\longrightarrow \text{Spacing between bursts}\end{aligned}$$

This difference between the time-scale for bursts and background fluctuations is not physically meaningful in general. This has the effect of overshooting the burst contribution to turbulent dispersion, which is estimated by the product of the probability  $\beta^{-1}$  of a burst, its time scale and the square of its velocity scale:

$$\beta^{-1} \times \beta\tau_E \times \beta u_T^2 = \beta u_T^2 \tau_E. \quad (A13)$$

(In comparison, the background contribution is  $u_T^2\tau_E$ , and, if the time-scales for burst and background were the same, the background and burst contributions would be identical).

## Appendix B: Spherical tensors and the SO(3) technique

A symmetric two-index tensor function can be decomposed in spherical tensors in the form

$$\delta^{ij}Y_l(\mathbf{x}), \quad \partial^i\partial^jY_l(\mathbf{x}), \quad x^ix^jY_l(\mathbf{x}), \quad (x^i\partial^j + x^j\partial^i)Y_l(\mathbf{x}) \quad (B1)$$

where  $Y_l(\mathbf{x})$  is an  $l$ -order polynomial in the components  $x_i$ :

$$Y_l(\mathbf{x}) = y^{i_1i_2\dots i_l}x_{i_1}x_{i_2}\dots x_{i_l} \quad (B2)$$

and  $y^{i_1 i_2 \dots i_l}$  is traceless with respect to any pair of indices [19]. From Eqn. (36), the  $l = 0$  and  $l = 2$  contributions to  $B^{ij}$  will have the form:

$$u_T B_0^{ij}(\mathbf{x}) = a|\mathbf{x}|\delta^{ij} + \hat{a}\frac{x^i x^j}{|\mathbf{x}|} \quad (B3)$$

$$\begin{aligned} u_t B_2^{ij}(\mathbf{x}) = & \frac{4b^{lm}}{|\mathbf{x}|} x_l x_m \delta^{ij} + 2c^{lm} |\mathbf{x}| \partial_i \partial_j x_l x_m + \frac{d^{lm}}{|\mathbf{x}|^3} x_l x_m x^i x^j \\ & + \frac{e^{lm}}{2|\mathbf{x}|} (x^j \partial^i + x^i \partial^j) x_l x_m \end{aligned} \quad (B4)$$

Applying the incompressibility condition  $\partial_i B^{ij} = 0$  leads to the equations:

$$\begin{cases} \hat{a} = -\frac{a}{3} \\ 8b^{lm} + 4c^{lm} + 8e^{lm} = 0 \\ 3d^{lm} - 4b^{lm} - e^{lm} = 0 \end{cases} \quad (B5)$$

Substituting the solution to Eqn. (B5) into Eqns. (B3-B4) leads to Eqn. (37).

In the case of a vector field, an analogous decomposition can be obtained in terms of spherical vectors in the form:

$$x^i Y_l(\mathbf{x}), \quad \partial^i Y_l(\mathbf{x}) \quad \text{and} \quad \epsilon^{ijk} x_j \partial_k Y_l(\mathbf{x}) \quad (B6)$$

If the vector field does not have an axial component, only the first two spherical vectors can contribute. If we have axial symmetry, identified by a direction  $\mathbf{u}$ , the tensors  $y^{i_1 i_2 \dots i_l}$  entering Eqn. (B2) will be zero trace symmetrized products of components  $u^i$  and of the identity matrix  $\delta^{ij}$ . The first spherical vectors  $x^i Y_l(\mathbf{x})$  and  $\partial^i Y_l(\mathbf{x})$  are respectively:

$$\mathbf{x}, \quad (\mathbf{u} \cdot \mathbf{x})\mathbf{x}, \quad \left( (\mathbf{u} \cdot \mathbf{x})^2 - \frac{1}{3}|\mathbf{u}|^2|\mathbf{x}|^2 \right)\mathbf{x} \quad (B7)$$

and

$$0, \quad \mathbf{u}, \quad (\mathbf{u} \cdot \mathbf{x})\mathbf{u} - \frac{1}{3}|\mathbf{u}|^2\mathbf{x} \quad (B8)$$

### Appendix C: Conditional random field statistics

We want to calculate conditional velocity moments in the form

$$\langle u^i(\mathbf{x}_0, t_0) u^j(\mathbf{x}_0, t_0) \dots | \mathbf{u}(\mathbf{x}_1, t_1), \mathbf{u}(\mathbf{x}_2, t_2), \dots \rangle \quad (C1)$$

Let us indicate, for  $l = 0, 1, \dots, n$ ,  $\mathbf{U}_l = \mathbf{u}(\mathbf{x}_l, t_l)$ , and  $\mathbf{C}_{lm} = \langle \mathbf{U}_l \mathbf{U}_m \rangle$ , assuming for simplicity a symmetric correlation tensor. For a Gaussian random field, the velocity correlations at points  $\{t_l, \mathbf{x}_l\}$  are obtained from the generating function

$$\tilde{\rho}(\{\boldsymbol{\eta}_l\}) = \exp\left(-\frac{1}{2} \sum_{l,m=0}^n \boldsymbol{\eta}_l \cdot \mathbf{C}_{lm} \cdot \boldsymbol{\eta}_m\right) \quad (C2)$$

Let us introduce the marginal PDF

$$\rho(\{\mathbf{U}_l, l = 1, \dots, n\}) = \mathcal{N} \exp\left(-\frac{1}{2} \sum_{l,m=1}^n \mathbf{U}_l \cdot \mathbf{D}_{lm} \cdot \mathbf{U}_m\right) \quad (C3)$$

where  $\mathcal{N}$  is the normalization and  $\mathbf{D}_{lm}$  is the inverse of the restriction of  $\mathbf{C}_{lm}$  to  $l, m = 1, \dots, n$ . We shall indicate in the following this restriction with a prime:

$$\sum'_{lm} \equiv \sum_{l,m=1}^n, \quad \{\mathbf{U}'_l\} \equiv \{\mathbf{U}_l, l = 1, \dots, n\}, \quad \text{etc.} \quad (C4)$$

The generating function for  $\mathbf{U}_0$  conditioned to  $\mathbf{U}_l, l = 1, \dots, n$  is obtained by inverse transforming  $\tilde{\rho}(\{\boldsymbol{\eta}_l\})$  with respect to  $\{\boldsymbol{\eta}'_l\}$  in  $\{\mathbf{U}'_l\}$  and dividing by the marginal PDF  $\rho(\{\mathbf{U}'_l\})$ :

$$\begin{aligned} \tilde{\rho}(\boldsymbol{\eta}_0 | \{\mathbf{U}'_l\}) &= \frac{1}{\rho(\{\mathbf{U}'_l\})} \int \prod'_l d^3 \eta_l \exp\left(-i \sum'_l \boldsymbol{\eta}_l \cdot \mathbf{U}_l \right. \\ &\quad \left. - \frac{1}{2} \sum'_{lm} \boldsymbol{\eta}_l \cdot \mathbf{C}_{lm} \cdot \boldsymbol{\eta}_m - \sum'_l \boldsymbol{\eta}_0 \cdot \mathbf{C}_{0l} \cdot \boldsymbol{\eta}_l - \frac{1}{2} \boldsymbol{\eta}_0 \cdot \mathbf{C}_{00} \cdot \boldsymbol{\eta}_0\right) \end{aligned} \quad (C5)$$

From here we can calculate the conditional moments in Eqn. (C1). We calculate first the mean velocity in  $\{t_0, \mathbf{x}_0\}$  given velocities  $\mathbf{U}_l$  in  $\{t_l, \mathbf{x}_l\} l = 1, \dots, n$ :

$$\begin{aligned} \langle \mathbf{U}_0 | \{\mathbf{U}'_l\} \rangle &= \frac{1}{\tilde{\rho}(0 | \{\mathbf{U}'_l\})} \frac{\partial \tilde{\rho}(\boldsymbol{\eta}_0 | \{\mathbf{U}'_l\})}{\partial i \boldsymbol{\eta}_0} \Big|_{\boldsymbol{\eta}_0=0} \\ &= \frac{\sum'_r \mathbf{C}_{0r}}{\rho(\{\mathbf{U}'_l\}) \tilde{\rho}(0 | \{\mathbf{U}'_l\})} \cdot \int \prod'_l d^3 \eta_l \boldsymbol{\eta}_r \exp\left(-\frac{1}{2} \sum'_{lm} \boldsymbol{\eta}_l \cdot \mathbf{C}_{lm} \cdot \boldsymbol{\eta}_m - i \sum'_l \boldsymbol{\eta}_l\right) \end{aligned} \quad (C6)$$

Carrying out the Gaussian integrals, we obtain the result:

$$\langle \mathbf{U}_0 | \{\mathbf{U}'_l\} \rangle = \sum'_{lm} \mathbf{C}_{0l} \cdot \mathbf{D}_{lm} \cdot \mathbf{U}_m \quad (C7)$$

The calculation of the second conditional moment is analogous and the result is:

$$\begin{aligned} \langle \mathbf{U}_0 \mathbf{U}_0 | \{\mathbf{U}'_l\} \rangle &= - \frac{1}{\tilde{\rho}(\boldsymbol{\eta}_0 | \{\mathbf{U}'_l\})} \frac{\partial^2 \tilde{\rho}(\boldsymbol{\eta}_0 | \{\mathbf{U}'_l\})}{\partial \boldsymbol{\eta}_0 \partial \boldsymbol{\eta}_0} \Big|_{\boldsymbol{\eta}_0=0} \\ &= \mathbf{C}_{00} - \sum'_{lm} \mathbf{C}_{0l} \cdot \mathbf{D}_{lm} \cdot \mathbf{C}_{m0} + \langle \mathbf{U}_0 | \{\mathbf{U}'_l\} \rangle \langle \mathbf{U}_0 | \{\mathbf{U}'_l\} \rangle \end{aligned} \quad (C8)$$

### Appendix D: Parameter determination in turbulent channel flow

The strong intermittency, related to the dynamics of streaks and bursts in the viscous sublayer and the buffer region, is taken into account by means of a bi-Gaussian PDF for the normal velocity (see Appendix A) [22, 23, 7], which affects the form of the drift term. Actually, the intermittency is not taken exactly along  $x_2^+$ , but along the direction identified by the eigenvector of  $R^{ij}$ , aligned with  $x_2^+$  at the walls. The deviation with respect to the normal direction reaches a maximum of about 15 degrees between the buffer and the logarithmic region.

At variance with purely Lagrangian models, the noise term in Eqn. (8) can include some geometric informations about turbulent structures. If quantitative informations were available on the structure functions, a possible strategy could be to carry out a linear fit with respect to the  $SO(3)$ ,  $SO(2)$  and streak parameters introduced in Section IV. The strategy that we follow here is more appropriate for situations in which only qualitative informations on the geometric structure of the large eddies are available. We first isolate the space part  $B^{ij}$  of the noise correlation [see Eqn. (35)] and partition it in contributions from the various coherent structures:

$$B_{ij} = h(x_2^+) \left( B_{ij}^{Streak} + B_{ij}^{SO(2)} + B_{ij}^{Burst} \right) + (1 - h(x_2^+)) B_{ij}^{Iso} \quad (D1)$$

where  $h$  is a weight function chosen in such a way that coherent structures are taken into account only in the near-wall region:  $h = 1$  for  $x_2^+ < 40$ ,  $h = 0$  for  $x_2^+ > 100$  and symmetric on the other wall. As regards time correlations, we assume that  $B_t^{ij}$  is proportional to  $R^{ij}$ , i.e.:

$$B_t^{ij} = \frac{2R^{ij}\Delta t}{u_T^2}. \quad (D2)$$

thus taking into account the strong anisotropy of the Reynolds tensor as the walls are approached. Back to the space component, trying to include all the turbulent

structures in an  $SO(3)$  noise model does not seem to work well near the wall, because of the large differences between correlation lengths and fluid velocity fluctuations in normal-to-the-wall direction with respect to the other directions [46] (see also Section IV). Likewise, trying to include streaks in the  $SO(2)$  component, as mentioned in section IV, results in a noise tensor not positive definite. We thus decompose the noise term in an  $SO(2) + \text{Streak}$  component in the plane  $(x_1, x_3)$ , going to zero far from the wall, and an  $SO(3)$  component including the  $x_2$  direction.

Approximating streaks as infinitely elongated structures, with transverse length-scale  $L_{Streak} = 5$  wall units at the wall, and growing up to 10 away from it, we can use Eqn. (43), which will take the form:

$$B_{11}^{Streak} = \frac{\tau_E}{u_T^2} (R_{11} - R_{33}) \frac{|\Delta x_3|}{L_{Streak}} \quad (D3)$$

This term accounts for all of the anisotropy  $R_{11} - R_{33}$  of the Reynolds tensor in the immediate vicinity of the wall. The isotropic part is taken into account by the  $SO(2)$  term:

$$B_{ij}^{SO(2)} = \frac{\tau_E}{u_T^2} (R_{33} - R_{22}) \frac{|\Delta \mathbf{x}|}{L_{SO(2)}} \left( \delta_{ij} - \frac{1}{2} \frac{\Delta x_i \Delta x_j}{|\Delta \mathbf{x}|^2} \right) \quad (D4)$$

and  $\Delta \mathbf{x}$  lies in the  $(x_1, x_3)$  plane. As for streaks, we choose a model for the correlation length  $L_{SO(2)} = 5$  at the wall and growing up to 20 wall units away from it.

Similarly to streaks, bursts are considered as infinitely long, aligned with  $x_2$ , and we model them using the expression for the axisymmetric vortices, Eqn. (40), derived in Section IV. The unphysical assumption of infinite length is corrected by the fact that at large distance from the wall, this contribution is killed by the factor  $h$  in Eqn. (D1) and the noise is dominated by the isotropic part  $B_{ij}^{Iso}$  (see next). The characteristic length  $L_{Burst}$ , transverse to burst axis, is taken equal to 5 at the wall and growing up to 20 wall units away from it. This corresponds to a value of the parameter  $a$  entering Eqn. (40) given by:

$$a_{Burst} = \frac{\beta R_{22} \tau_E}{u_T L_{Burst}} \quad (D5)$$

where  $\beta = \frac{2}{3} (R_{22})^{-2} \langle u_2^4 \rangle - 1$  [see Eqn. (A2)] accounts for the effect of intermittency. As discussed at the end of Section IV and in Appendix A, the dispersion in the direction of the intermittent velocity is dominated by the bursts and the factor  $\beta$  is necessary to have the time scale for these bursts set to  $\tau_E$  rather than to  $\beta \tau_E$ .

Finally, in the core region the turbulent structures are nearly isotropic and the isotropic form of the noise, provided by Eqn. (38), has been adopted, with the same value of the parameter  $a$  used in the section IX:  $a_{iso} = 0.65$ .

We are left with the analysis of the gauge term  $\Xi$ . Due to symmetry of the flow, the only contributions are the time component described in Eqn. (50), and the strain contributions to the space component  $\bar{\xi}_1^3$  and  $\bar{\xi}_2^3$ , given by Eqn. (54). We have decided to keep only the time component, that is in some way associated with the ejection process: choosing  $\xi_0^3 = u_T^2$  at the  $x_2 = 0$  and vanishing at  $x_2 = 40$  (and same profile with changed sign at the opposite wall). This contribution appears to be related to the streak lifting process: regions near the wall moving more slowly than the fluid tend in fact, on the average, to rise.